Molecular Design of Single Site Catalyst Precursors for the Ring-Opening Polymerization of Cyclic Ethers and Esters. 2.[1] Can Ring-Opening Polymerization of Propylene Oxide Occur by a Cis-Migratory Mechanism?†

Björn Antelmann, Malcolm H. Chisholm,* Suri S. Iyer, John C. Huffman, Diana Navarro-Llobet, and Marty Pagel

Department of Chemistry, Indiana University, Bloomington, Indiana 47405

William J. Simonsick and Wenqing Zhong

E. I. DuPont, Marshall R and D Laboratory, Philadelphia, Pennsylvania 19146

Received February 8, 2001

ABSTRACT: From the reactions between 2,2′-ethylidenebis(4,6-di-*tert*-butylphenol) and 2,2′-methylidenebis(4-dimethyl-6-di-*tert*-butylphenol) and Et_2AlCl the biphenoxide complexes $[(O{\sim\sim}CHMe{\sim\sim}O)AlCl]_2$, **1**, and $[(O{\sim\sim}CH_2{\sim\sim}O)AlCl]_2$, **2**, have been isolated and characterized. These dimers are broken up by donor ligands, and the molecular structure of ethylidenebis(4,6-di-*tert*-butylphenoxide)AlCl(THF), **3**, has been structurally characterized. Racemic 5,5′-6,6′-tetramethyl-3,3′-di-*tert*-butyl-1,1′-biphen-2,2′-diol and Et_2AlCl react in hexane to give $[(O{\sim\sim}O)AlCl]_2$, compound **6**, as a hydrocarbon insoluble white precipitate. In the donor solvent THF monomeric species are formed, and (O∼∼O)AlX(THF) has been crystallographically characterized, X = 20% Cl and 80% Et occupancy. Refluxing in THF favors X = Cl, compound **4**. The reaction of $Et_2Al(OEt)$ with the biphenol gives (O∼∼O)AlEt(THF), **5**, in the presence of THF by displacement of one ethyl and one ethoxide ligand. Compounds **1**, **2**, **3, 4, 5, 6,** $[(O{\sim\sim}CHMe{\sim\sim}O)Al(O^iPr\text{-}d_7)]_2$, and $[Cp_2Zr(OEt)(OEt_2)]^+[HB(C_6F_5)_3]^-$ act as propylene oxide, PO, polymerization catalyst precursors. The polymers have been examined by MS techniques and NMR spectroscopy, and these results are compared with polypropylene oxide, PPO, formed by base catalysis and by porphyrin- and salen-AlCl catalyst precursors. The new Al compounds and the cationic zirconium alkoxide give close to 50:50 HH to TT junctions with end groups C−Cl, OH, and $=CH_2$ being identified by MS and NMR. Polymerizations employing $[(O{\sim\sim}CHMe{\sim\sim}O)Al(O^iPr\text{-}d_7)]_2$ give $HO{-}(PO)n{-}O^iPr\text{-}d_7$ oligomers, in addition to vinyl-terminated species. Polymerization of *S*-PO and 50:50 mixtures of *S*-PO and *rac*-PO reveals that the stereoirregular polymer is formed by a stereoselective ring-opening step. An analysis of the HH and TT junctions at the triad level is made, extending the earlier assignments of Tonelli and Schilling. This analysis leads us to suggest that polymerization occurs by a cationic coordinate mechanism wherein ring opening occurs by backside attack on an activated PO molecule which leads to inversion at the methine carbon. The *rac*-biphenoxide−Al complexes show a preference for **ii** and **i** linkages in (HT)(HT)(HT) units. These results are compared to coordinate catalysis polymerizations of PO employing the Union Carbide calcium amide−alkoxide system and (porphyrin)AlCl and lead us to predict that a cis-migratory ring-opening polymerization process is not likely to be developed for polymerization of PO.

Introduction

In contrast to the remarkable advancements in single-site polyolefin synthesis that have been made over the past two decades,[2] the synthesis of polyoxygenates derived from ring-opening polymerization, ROP, of alkene oxides, cyclic ethers, and cyclic esters has progressed more slowly and received little general attention. In part 1 of this series, we examined the reactivity of L_nMOR compounds, where M = Mg and Zn and L_n was a η^3-trispyrazolyl borate or indazolyl borate ligand.[1] These were active in ROP of lactides and lactones, and studies of kinetics revealed that these polymerizations were first order in metal complex and substrate. Furthermore, these polymerizations were living and gave narrow polydispersities up to 90% polymerization. Although the magnesium catalyst precursors were among the most active of all known coordinate catalysts,[3] second only to the activity of certain lanthanide alkoxides (which are not single-site catalysts) reported by workers from DuPont,[4] they failed to show any activity toward the polymerization of PO under ambient conditions. This lack of activity was notable because other zinc alkoxides derived from reactions of $ZnEt_2$[5] and various alcohols are known to be active in ROP of PO as are simple bases such as OH− and OR− with group 1 metal countercations.[6] Ring opening of PO is well-known to occur by backside attack in organic chemistry[7] though there are certain well-documented examples of cis-ring opening by Lewis acid promoters such as $AlCl_3$.[8] Thus, a question that naturally arose from our earlier work was whether the use of bulky η^3-LMOR metal complexes which, though active for ROP of lactide by a cis-migratory insertion process, were inactive to PO because the cis-migratory insertion process was not favored for PO. Alternatively, was it merely that these metal centers were not sufficiently Lewis acidic?

† Dedicated to Dr. Walter Reichle, Corporate Research Fellow, Union Carbide, on the occasion of his retirement.

* Corresponding author. E-mail Chisholm@chemistry.ohio-state.edu.

10.1021/ma0102316 CCC: $20.00
Published on Web 04/05/2001

Scheme 1. Two Possible Modes of Ring Opening of Epoxides in Coordinate Catalysis

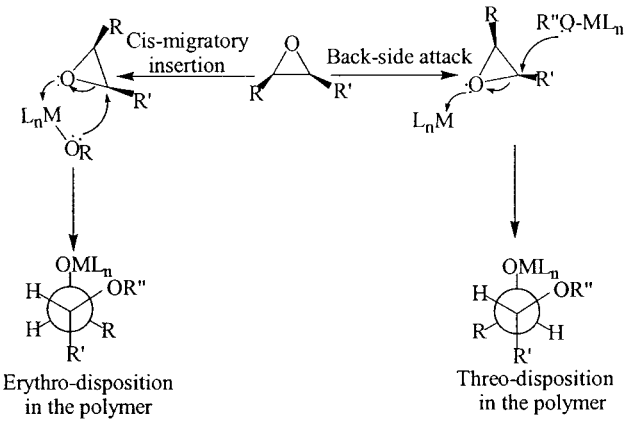

Coordination complexes of Al(3+) such as (porphyrin)-AlX,[9] where X = Cl, OR, SR, and related (salen)AlX [10] complexes are active in ROP of PO. Indeed, from the extensive work of Inoue, we know that the (porph)AlOP system is living or immortal in its polymerization of PO. [9] However, there is extensive evidence from the use of this catalyst precursor system with other substrates that the ring-opening process involves backside attack. This is known from studies of the stereochemistry of ring-opening of the substrate 2,3-epoxybutane [11] and from the kinetics of the ROP of δ-valerolactone[12] where the reaction was found to be first order in substrate and second order in [Al]. Also, it was shown that Lewis acid additives such as BPh_3 accelerate ROP of PO by the (porph)Al(OP).[13]

We thus were caused to question the mechanism of ring-opening polymerization of PO by coordinate catalysis. The two most likely possibilities are compared in Scheme 1 where it is shown that they are in principle distinguishable by their stereochemical outcome. However, for PPO with a stereoregular (HTHTHT) backbone NMR spectroscopy cannot be used to discriminate between erythro and threo junctions[14] (Scheme 1). Even specific isotopic labeling of *S*-Me[CH−CHD−O] would be not useful as the 2*J* ^{1}H resolved spectrum of PPO is known to give J_{HH} values that are insufficiently sensitive to be informative with regard to polymer conformation.[15] It is from insight into a stereoirregular polymer containing HH, TT, and $(HT)_n$ junctions that stereochemical information can be gleaned from NMR studies.

Aside from an academic interest in the various possibilities for ROP of PO, it should be recognized that PPO and its low molecular weight polyols find a huge commodity market of ca. 10^6 metric tons per annum in the USA alone.[16] Applications include their use as flocculants,[17] water- and ion-soluble polymers,[17] reactants with isocyanates in the synthesis of urethane polymers[17] and in the synthesis of elastomers such as Spandex and Lycra,[18] and even specialty biocompatible polymers.[19] High molecular weight polyethers, PEO and PPO, are commonly made by the Union Carbide heterogeneous process employing a so-called calcium amide−alkoxide catalyst,[20] the mechanism of which is not known, at least within the public domain. The use of the Inoue (porph)AlX system shown in **A** gives very high molecular weight polymers, but it is not commercially attractive because (1) the porphyrin imparts color to the PPO and (2) the PPO is not readily separated from the (porph)Al center.

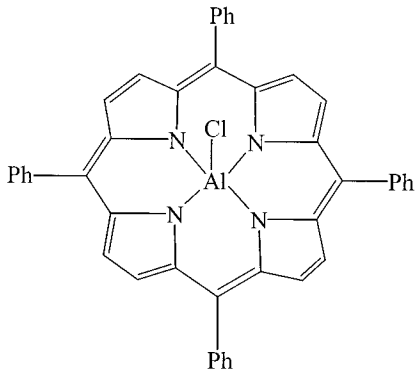

A

A catalyst system with a planar ligand such as a porphyrin and to some extent a salen ligand (although the latter is certainly more flexible) does not endear itself to a cis-migratory insertion mechanism since the cis-coordination site at the metal center is relatively inaccessible. We therefore determined to prepare a series of aluminum(3+) complexes where cis-migratory ring opening would be favored on steric grounds. In particular, we were attracted to the use of chelating 2-(doubly negative charged) ligands such as the biphenoxides and the binolate shown in **B**, **C**, and **D**. The

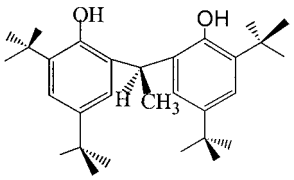

B

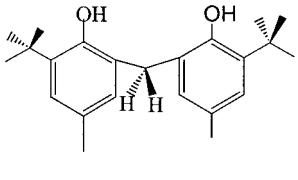

C

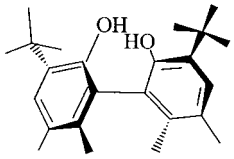

D (rac)

use of chelating ligands should suppress deleterious ligand scrambling reactions which would occur for monodentate alkoxide or phenoxide ligands, and by the judicious choice of substituents one could control the steric access to the metal center and the coordination environment at Al(3+). The compounds 2,2′-ethylidenebis(4,6-di-*tert*-butylphenol), **B**, and 2,2′-methylidenebis(4-dimethyl-6-di-*tert*-butylphenol), **C**, represented as HO∼∼CHMe∼∼OH and HO∼∼CH_2∼∼OH hereafter for brevity, are readily available and inexpensive as they find industrial uses as antioxidants. The racemic 5,5′-6,6′-tetramethyl-3,3′-di-*tert*-butyl-1,1′-biphen-2,2′-diol, **D**, denoted hereafter as HO∼∼OH, is also commercially available and is fairly readily resolved should the need arise. This ligand has been used by Schrock and co-workers in stereoselective olefin metathesis reactions.[21]

We describe here our use of these ligands in the synthesis and characterization of new Al(3+) complexes and their use in ROP of PO together with details of a

stereochemical analysis of the PPO. These results are discussed in terms of the earlier work of Inoue, Tsuruta, and Union Carbide in the formation of PPO and in polymer microstructure analysis based on the pioneering work of Schilling and Tonelli.[22]

Results and Discussion

Preparations of Aluminum Biphenoxide and Binolate Complexes. The reactions between the biphenols shown in **B** and **C** and hydrocarbon solutions of Et_2AlCl give white, hydrocarbon-soluble crystalline ethylidene and methylidene biphenoxides, $[(O\sim\sim CHMe\sim\sim O)AlCl]_2$, **1**, and $[(O\sim\sim CH_2\sim\sim O)AlCl]_2$, **2**. The ^1H NMR data for **1** and **2** in toluene-d_8 and benzene-d_6 are consistent with a dimeric structure in solution wherein the biphenoxide ligand is μ-η^1-η^2-coordinated, and each half of the molecule is related by C_2 symmetry. The structural characterization of **1** supports this view, and significantly the NMR data indicate the presence of only one possible isomer in solution.

The dimeric structure of **1** or **2** is broken in the presence of donor ligands, L, such as THF to give complexes (O∼∼CHR∼∼O)AlCl(L), where R = H or Me, and the solid-state structure of (O∼∼CHMe∼∼O)AlCl-(THF), **3**, is described later. The NMR data in toluene-d_8 indicate that the ligation of the THF molecule is maintained in hydrocarbon solutions.

The reaction between the substituted binol and Et_2AlCl in hexane leads to a hydrocarbon insoluble precipitate formulated as $[(O\sim\sim O)AlCl]_2$, **6**, based on elemental analysis and crystallographic characterization. This is soluble in THF and forms a white crystalline compound [(O∼∼O)AlCl(THF)]. Rather interestingly, when the reaction between the binol and Et_2AlCl is carried out in THF as solvent, the replacement of the Al−Et bond is more sluggish and the Al−Cl bond is kinetically more labile toward the reversible elimination of HCl. At ambient temperatures and even with heating to +60 °C, a white crystalline material [(O∼∼O)AlX-(THF)] can be obtained after recrystallization, where $X = Et_x, Cl_{1-x}$. Crystals were examined by single-crystal X-ray crystallography and revealed that the two compounds (O∼∼O)AlEt(THF) and (O∼∼O)AlCl(THF) cocrystallize as (O∼∼O)AlX(THF), where X = 80% Et and 20% Cl. The reaction between Et_2AlCl and the substituted binol in THF at 80 °C for 4 h leads to complete elimination of the Al−Et bond and formation of [(O∼∼O)AlCl(THF)], compound **4**.

Rather interestingly, the reaction between the substituted binol, **D**, and Et_2AlOEt leads to [(O∼∼O)AlEt-(THF)], **5**, by the elimination of ethane and ethanol. The Al−Et bond in **5** is inert to reaction with EtOH to give [(O∼∼O)AlOEt(THF)]. Thus, in the binolate complexes we have access to pure [(O∼∼O)AlX(THF)], where X = Cl, **4**, and Et, **5**, though mixtures of the two cocrystallize and are generally formed in reactions between Et_2AlCl and the binol **D** in the solvent THF. These compounds therefore differ in regard to coordination number from the cationic Lewis acid Al complexes recently reported by Atwood.[23]

Solid-State and Molecular Structures. *$[(O\sim\sim CHMe\sim\sim O)AlCl]_2$*, **1**. An ORTEP drawing of the dimeric compound **1** is shown in Figure 1. The bulky 2,2′-ethylidenebis(4,6-di-*tert*-butylphenoxide) ligand forms an eight-membered ring to Al(1), and one oxygen atom, O(3), bridges to the other aluminum atom, Al(1)′. The μ-η^1-η^2 mode was seen in a related zirconium complex

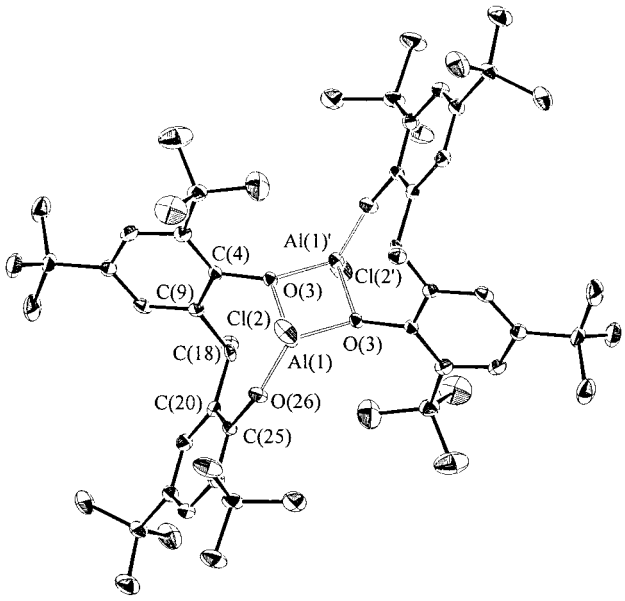

Figure 1. ORTEP view of the dimer $[(C_{30}H_{44}O_2)AlCl]_2$ (**1**) showing the atom numbering scheme.

Table 1. Selected Bond Distances (Å) and Angles (deg) for Compound 1

Al(1)−Cl(2)	2.081(1)	Al(1)−O(3)−Al(1)	98.5(1)
Al(1)−O(3)	1.822(3)	O(3)−Al(1)−O(3)	81.5(1)
Al(1)−O(3)	1.823(2)	Al(1)−O(3)−C(4)	136.0(2)
Al(1)−O(26)	1.662(3)	Al(1)−O(3)−C(4)	120.03(2)
O(3)−C(4)	1.434(4)	Al(1)−O(26)−C(25)	157.2(2)
O(26)−C(25)	1.361(4)	Cl(2)−Al(1)−O(3)	114.76(9)
C(4)−C(9)	1.389(5)	Cl(2)−Al(1)−O(3)	112.62(9)
C(9)−C(18)	1.521(5)	Cl(2)−Al(1)−O(26)	109.3(1)
C(18)−C(20)	1.515(5)	O(3)−Al(1)−O(26)	113.4(1)
C(20)−C(25)	1.392(5)	O(3)−Al(1)−O(26)	123.0(1)
		O(26)−C(25)−C(20)	118.8(3)
		O(3)−C(4)−C(9)	116.4(3)
		O(4)−C(9)−C(18)	125.0(3)

$[Zr(O\sim\sim CHMe\sim\sim O)_2]_2$.[24] The molecule has a C_2 axis of symmetry which relates the coordination spheres of each Al center. The Al(O∼∼CHMe∼∼O) eight-membered ring is puckered, forming a rooflike structural motif, and the C−Me moiety and Al−Cl bond are anti to one another. Selected bond distances and bond angles are given in Table 1. As expected, the Al−O(26) terminal distance, 1.66(1) Å, is notably smaller than the bridging Al−O(3) bond distance, 1.82(1) Å. The coordination about Al is readily seen to be that of a distorted tetrahedron with the largest angle being associated with the eight-membered ring of the biphenoxide ligand.

(O∼∼CHMe∼∼O)AlCl(THF), **3**. An ORTEP drawing of the monomeric compound **3** is shown in Figure 2. Once again, we see the puckered or roof-shaped eight-membered ring of the 2,2′-ethylidenebis(4,6-di-*tert*-butylphenoxide), and again the Al−Cl and C−Me bonds are anti. Selected bond distances and bond angles are given in Table 2. The Al−O(3) bond distance, 1.94(1) Å, associated with the coordinated THF bond is notably longer than Al−O biphenoxide distances, 1.72(2) Å (average), as might be expected for a dative bond. It is, however, shorter than the Al−O bridging distances in **1** (Table 1). The angles of the bonds subtended at Al are all distorted from the idealized tetrahedral angle with the largest being associated with the eight-membered ring of the biphenoxide, 123°, and the smallest being that between the Al−Cl and the Al−O(THF) bond, 94.5°. The latter is significant in that as a model

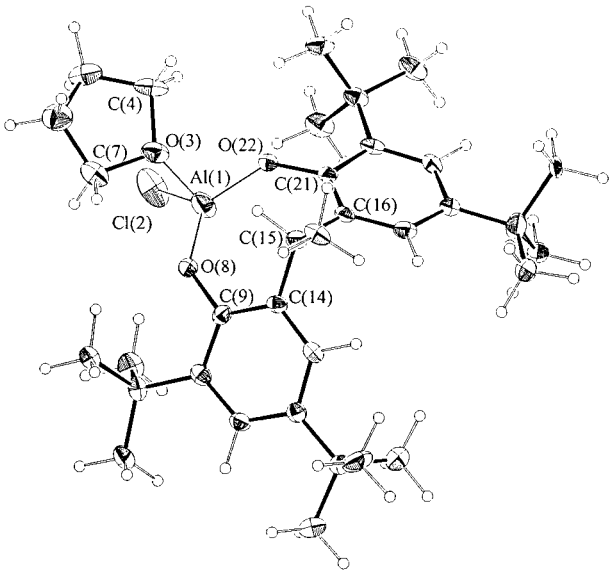

Figure 2. ORTEP view of the monomer $[(C_{30}H_{44}O_2)AlCl(THF)]$ (**3**), showing the cis disposition between the chlorine atom and the THF molecule and the atom numbering scheme.

Table 2. Selected Bond Distances (Å) and Angles (deg) for Compound 3

Al(1)−Cl(2)	2.110(2)	Cl(2)−Al(1)−O(3)	94.5(1)
Al(1)−O(3)	1.936(3)	Cl(2)−Al(1)−O(8)	115.5(1)
Al(1)−O(8)	1.715(3)	Cl(2)−Al(1)−O(22)	119.7(1)
Al(1)−O(22)	1.711(3)	O(3)−Al(1)−O(8)	94.9(1)
O(3)−C(4)	1.481(5)	O(3)−Al(1)−O(22)	92.7(1)
O(3)−C(7)	1.470(4)	O(8)−Al(1)−O(22)	123.3(1)
O(8)−C(9)	1.357(4)	Al(1)−O(3)−C(4)	118.8(2)
O(22)−C(21)	1.360(4)	Al(1)−O(3)−C(7)	119.3(2)
C(9)−C(14)	1.412 (5)	C(4)−O(3)−C(7)	108.6(3)
C(14)−C(15)	1.531(5)	Al(1)−O(8)−C(9)	136.2(2)
C(15)−C(16)	1.531(5)	Al(1)−O(22)−C(21)	133.9(2)
C(16)−C(21)	1.405(5)	O(8)−C(9)−C(14)	119.8(1)
		O(22)−C(21)−C(16)	120.1(3)

for a single-site catalyst system for cis-migratory ring opening the Al−O(THF) bond would represent the site for an entering epoxide and the Al−Cl bond the site of the Al−O bond for the growing polymer chain (OP). Steric factors associated with this bulky biphenoxide clearly will force the substrate and OP group into close proximity.

(O∼∼O)AlX(THF), where X = 80% Et and 20% Cl. We introduce this structure, even though the occupancy of the X site is 4:1 for Et:Cl because it serves to describe the salient structural features for (O∼∼O)AlCl(THF), **4**, and (O∼∼O)AlEt(THF), **5**, both of which can be isolated in a pure form. Two views of one of the enantiomers found in the crystal are shown in Figure 3. These views emphasize once again the pseudotetrahedral geometry about the aluminum center and the C_2 symmetry of the 5,5′-6,6′-tetramethyl-3,3′-di-*tert*-butyl-1,1′-biphen-2,2′-diolate ligand. Selected bond distances and bond angles are given in Table 3. Though Al−X distances may prove unreliable (as is now well accepted for so-called bond stretch isomers where Cl and O atoms have partial occupancy factors), the other distances and angles listed in Table 3 should be taken as reliable. Once again the Al−O(THF) bond distance, 1.86(1) Å, is notably longer than the Al−O binolate bond distances, 1.74(1) Å. The angles subtended at Al are distorted from the idealized tetrahedral angle, ranging from 125° to 96°. The (THF)O−M−X angle is 106°.

$[(O∼∼O)AlCl]_2$, **6**. An ORTEP drawing of the dimeric compound **6** is shown in Figure 4. The structure of this

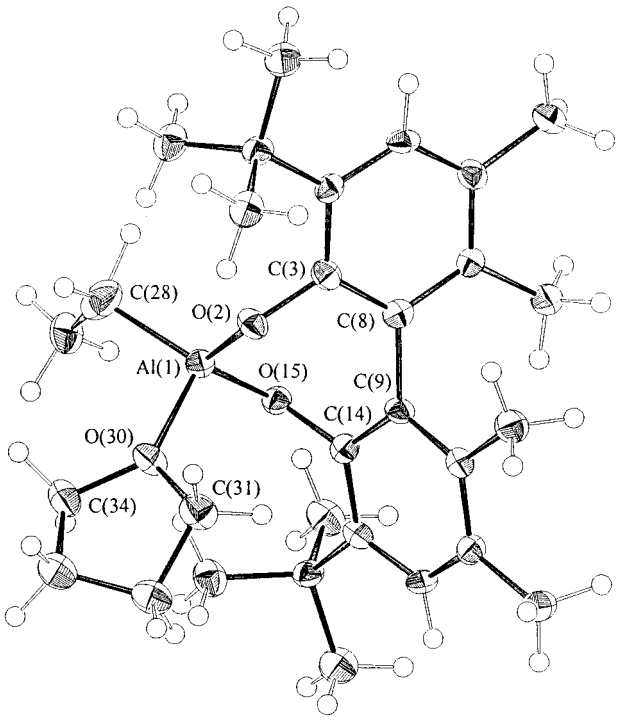

Figure 3. ORTEP view of the monomer $[(C_{24}H_{32}O_2)AlCl_{0.2}ethyl_{0.8}(THF)]$ (**4**), giving the atom numbering scheme. Only X = Et is shown.

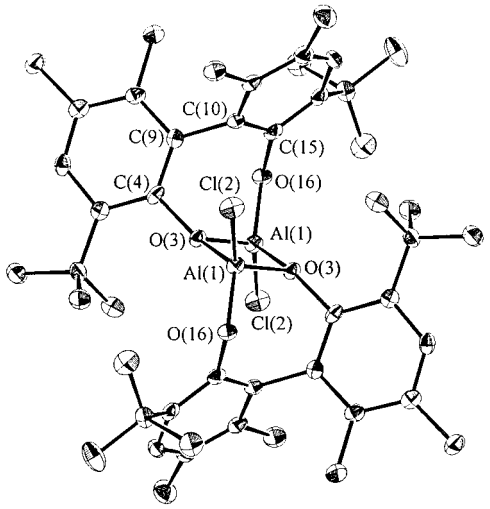

Figure 4. ORTEP view of the dimer $[(C_{24}H_{32}O_2)AlCl]_2$ (**6**), giving the atom numbering scheme.

Table 3. Selected Bond Distances (Å) and Angles (deg) for Compound 4

Al(1)−C(28)	2.036(3)	O(2)−Al(1)−O(15)	110.1(1)
Al(1)−O(2)	1.738(2)	O(2)−Al(1)−O(30)	95.8(1)
Al(1)−O(15)	1.744(2)	O(2)−Al(1)−C(28)	123.6(1)
Al(1)−O(30)	1.858(2)	O(15)−Al(1)−O(30)	108.6(1)
O(2)−C(3)	1.373(4)	O(15)−Al(1)−C(28)	110.4(1)
O(15)−C(14)	1.372(3)	O(30)−Al(1)−C(28)	106.4(1)
O(30)−C(31)	1.491(4)	Al(1)−O(2)−C(3)	117.2(2)
C(3)−C(8)	1.409(4)	Al(1)−O(15)−C(14)	116.1(2)
C(8)−C(9)	1.514(4)	Al(1)−O(30)−C(31)	122.0(2)
C(9)−C(14)	1.407(4)	Al(1)−O(30)−C(34)	128.0(2)
O(30)−C(34)	1.467(4)	O(2)−C(3)−C(8)	118.2(3)
		O(15)−C(14)−C(9)	118.8(3)

compound is closely related to that of compound **1**. The molecule has a center of inversion, and each enantiomer of the racemic 5,5′-6,6′-tetramethyl-3,3′-di-*tert*-butyl-1,1′-biphen-2,2′-diolate is present in the molecule. Se-

Table 4. Selected Bond Distances (Å) and Angles (deg) for Compound 6

Al(1)−Cl(2)	2.086(1)	Al(1)−O(3)−Al(1)	99.6(1)
Al(1)−O(3)	1.836(2)	O(3)−Al(1)-O(3)	80.4(1)
Al(1)−O(3)	1.837(2)	Al(1)−O(3)−C(4)	117.8(2)
Al(1)−O(16)	1.717(2)	Al(1)−O(3)−C(4)	133.2(2)
O(3)−C(4)	1.441(4)	Al(1)−O(16)−C(15)	120.7(2)
O(16)−C(15)	1.373(4)	Cl(2)−Al(1)−O(3)	111.15(9)
C(4)−C(9)	1.401(5)	Cl(2)−Al(1)−O(3)	126.4(1)
C(9)−C(10)	1.516(5)	Cl(2)−Al(1)−O(16)	108.5(1)
C(10)−C(15)	1.407(5)	O(3)−Al(1)−O(16)	124.0(1)
		O(3)−Al(1)−O(16)	105.6(1)
		C(4)−C(9)−C(10)	125.2(3)
		C(9)−C(10)−C(15)	117.5(3)
		O(3)−C(4)−C(9)	116.5(3)
		O(16)−C(15)−C(10)	118.7(3)

lected bond distances and angles are given in Table 4, and a summary of the crystallographic data for all the compounds reported herein is given in Table 5. As seen for compound **1**, the coordination about Al is that of a distorted tetrahedron, and Al−Cl bonds are also anti to one another.

Solution and Other Characterization Data. By far the most informative characterization data for these new white, hydrocarbon-soluble compounds comes from NMR studies. All of the compounds show essentially temperature-independent NMR spectra, and in each case the NMR data support the structural data found in the solid state by X-ray crystallography. For example, in the ^{1}H NMR spectrum of **1** there are four ^{t}Bu signals of equal intensity and one CMe doublet and one CH quartet for the ethylidene moiety. Clearly, only one isomer having C_2 symmetry is present in solution, and the NMR data support the μ,η^1,η^2 mode of binding for the O∼∼CHMe∼∼O ligand. Similarly for **2**, there are two ^{t}Bu singlets and two Me singlets, and the methylidene protons appear as an AX spectrum. The conformation within the eight-membered rings is rigid on the NMR time scale. For the binolate AlEt(THF) complex **5**, the methylene protons of the ethyl ligand are diastereotopic and are thus part of an ABX_3 spin system.

One point of puzzlement to us is the consistently low carbon elemental analysis found for the diolate compounds. See Experimental Section. This is particularly puzzling since the H and Cl (and even the O when determined) are all within the anticipated range. We have no explanation for this fact, but we have no doubt that, on the basis of the spectroscopic data and the crystal structures, these compounds are well represented as described above and are readily purified by crystallization, with the exception of the (O∼∼O)AlX(THF) compounds, where X = Cl and Et, which cocrystallize. For the latter the presence of two compounds is evident from ^{1}H NMR spectroscopy.

Polymerization Studies Involving Propylene Oxide. General Comments. The compounds **1**, **2**, **3**, **4**, **5**, and **6** all act as catalyst precursors for the polymerization of propylene oxide, PO. We have examined the polymers formed by the addition of PO to solid samples of the aluminum complexes where the PO:Al ratio is ca. 200−300:1, and we have also followed the polymerization reactions by NMR spectroscopy in benzene-d_6 or toluene-d_8. The dimeric compounds **1** and **2** in toluene-d_8 are seen to be cleaved into (O∼∼CHMe∼∼O)AlCl(L) and (O∼∼CH_2∼∼O)AlCl(L), where L = PO or THF, in the presence of added PO and THF. Free and coordinated PO are in rapid dynamic exchange. By ^{1}H NMR spectroscopy the resonances of the biphenoxide are relatively insensitive to the nature of the Al−Cl or Al−OP group, where OP = the growing polypropylene oxide chain.

In the case of the binolate complexes **4** and **5**, PO competes with THF for binding to the Al center. In this instance, for **5**, the loss of the Al−Et bond is readily apparent from ^{1}H NMR studies.

The PPO prepared in bulk polymerizations is in all cases very similar for the aluminum catalyst precursors **1** and **2**. The PPO samples derived from the binolate complexes **4** and **5** are similar to each other and have a lower viscosity than the PPO derived from **1** and **2**. The former have a marked preference for isotactic junctions (vide infra). Since the primary focus of this work was to elucidate the stereochemistry of the ring-opening event from a examination of the microstructure of the PPO, we have carried out a series of reactions, each involving **1**, **2**, **4, 5,** or **6** and PO, and compared these to polymerizations involving the use of Inoue's catalyst (TPP)AlCl, where TPP = tetraphenylporphyrin, and the Union Carbide catalyst system employing so-called calcium−amide−alkoxide.

In addition to the [Al−Cl] bond initiated polymerizations noted above, which we presume lead to growing [Al−OP] chains with terminal C−Cl bonds, we investigated the use of the deuterated isopropoxide complex [(O∼∼CHMe∼∼O)Al(O^{i}Pr-d_7)]$_2$, which has recently been reported and structurally characterized in its protio form, [25] in order to interrogate the nature of the end groups and to gain information concerning the mechanism of the ring-opening process and other reactions leading to chain transfer.

Table 5. Summary of Crystal Data for Compounds 1, 3, 4, and 6

	compd **1**	compd **3**	compd **4**	compd **6**
empirical formula	$C_{60}H_{88}Al_2Cl_2O_4$·$2C_7H_8$	$C_{36}H_{56}AlClO_{3.5}$·0.5THF	$C_{29.6}H_{44}AlCl_{0.2}O_3$	$C_{48}H_{64}Al_2Cl_2O_4$·$2C_6H_6$
fw	1182.51	607.27	480.67	986.13
space group	*Pcab*	*P*$\bar{1}$	*P*21/*n*	*P*21/*c*
a (Å)	18.748 (4)	13.341(2)	7.851 (1)	12.495 (0)
b (Å)	20.207 (4)	13.882(2)	20.198 (3)	21.595 (1)
c (Å)	18.372 (4)	11.045(1)	17.916 (2)	10.173 (0)
α (deg)	90.00 (0)	105.62(1)	90.00 (0)	90.00 (0)
β (deg)	90.00 (0)	95.19(1)	97.61 (0)	101.13 (0)
γ (deg)	90.00 (0)	62.75 (1)	90.00 (0)	90.00 (0)
temp (K)	100	98	112	114
Z	4	2	4	2
V (Å)	6960.05	1750.12	2816.14	2693.28
D_{calc} (g cm^{-1})	1.129	1.152	1.134	1.216
λ (Å)	0.710 69	0.710 69	0.710 73	0.710 73
μ (cm^{-1})	1.642	1.678	0.993	1.989
R (F)	0.068	0.0568	0.035	0.062
Rw (F)	0.049	0.0575	0.027	0.077

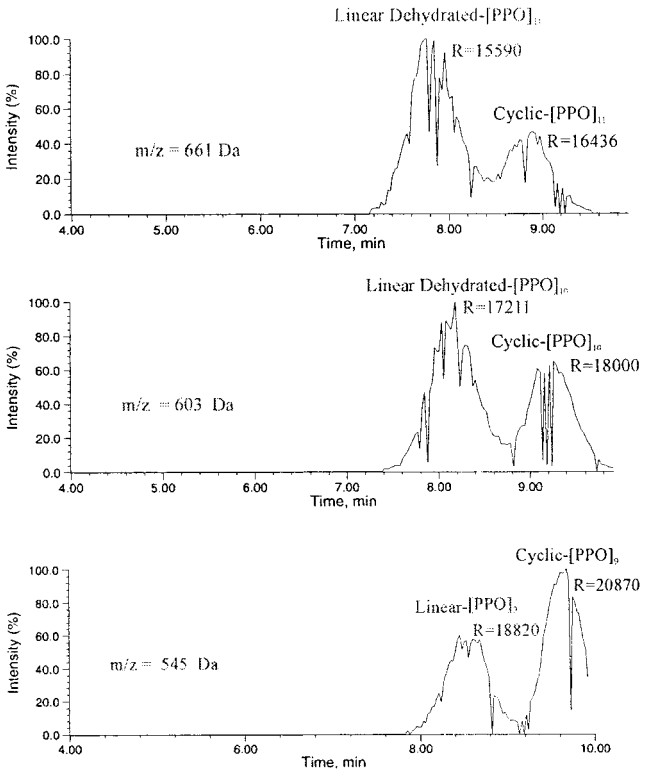

Figure 5. Selected oligomer profiles of isomers separated by GPC/FTMS.

We also examined the reactivity of a cationic zirconium alkoxide complex, [26] $[Cp_2Zr(OEt)(OEt_2)]^+[HB(C_6F_5)_3]^-$, which, like the neutral (biphenoxide)AlX(THF) complexes previously described, contains cis M−OR and M−O(ether/substrate) binding sites. The use of the zirconium complex makes a full analogy with the now well-documented cis-migratory insertion of alkenes into metal−alkyl bonds in cationic metallocene α-olefin polymerization.[2]

Polymer Characterization by Mass Spectrometry. PPO's derived from reactions involving PO and **1** and **2** contain cyclic oligomers and linear chains. The cyclic oligomers of lower molecular weight can be removed by vacuum distillation while the high molecular weight cyclic oligomers, e.g., $(OCH_2CHMe)_{15}$, can be detected by GPC/MS since their retention times differ with the cycles coming off the column first. This is shown in Figure 5. NMR analysis showed the presence of propenyl-terminated oligomers of formula $[C_3H_6O]_n$, which accounted for <10% of the oligomer distribution. However, their abundance, based upon the LD/FTMS data, calculated to >30 mol %. Cyclic oligomers formed under the polymerization conditions, which would also have the formula $[C_3H_6O]_n$. Although single-stage soft ionization mass spectrometry will not distinguish these species because they have identical molecular formulas, GPC in conjunction with soft ionization mass spectrometry can resolve isomers provided that the isomeric materials differ in their hydrodynamic size. Therefore, we used GPC/FTMS to characterize the oligomers. The elution behavior of the mono-sodiated ions 545, 603, and 661 Da shown in Figure 5 reveals the selected oligomer profiles of the 9−11-mers. As expected, the larger oligomers elute first followed by the smaller oligomers, i.e., the 11-mers elute prior to the nonamers. We observe two well-resolved peaks for each ion. Furthermore, the relative abundance of the later eluting peak (smaller size) decreases with increasing chain length.

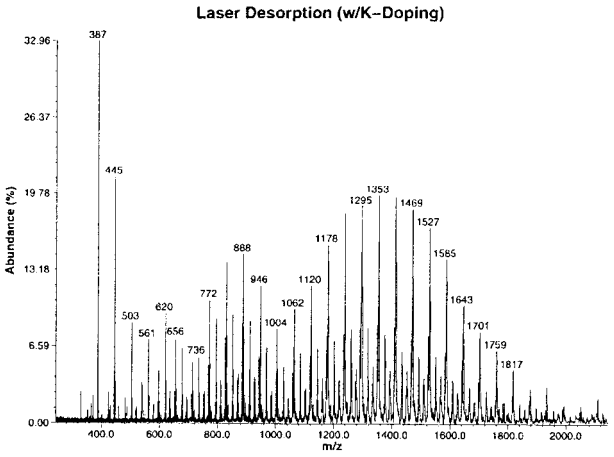

Figure 6. Molecular weight distribution of a linear polymer by laser desorption (w/K-doping).

From the LD/FTMS studies shown in Figure 6, we know that the linear polymers have a fairly broad molecular weight distribution spanning 1000−4000 Da. Under our LD/FTMS conditions the organic molecules are vaporized, and the neutral species undergo an ion−molecule reaction with potassium leading to the formation of mono-potassiated adduct ions. Several distributions are evident as seen by the numerous spacings of 58 Da, corresponding to the mass of the propylene oxide repeat unit $[C_3H_6O]$. The base peak is seen at 387 Da. Subtracting the mass of potassium from the 387 Da ion yields a mass of 348 Da, corresponding to $[C_3H_6O]_6$. We attribute the 387 ion to propenyl-terminated oligomers that could have been formed via dehydration of hydroxyl-terminated propylene oxide. The ions seen at 445, 503 Da, ... are due to additional units of propylene oxide. The abundant distribution extending from approximately 500 Da through 2000 Da and maximizing at 1353 Da has a relatively large M + 2 isotope peak supporting a mono-chlorinated oligomer which was also observed in the NMR spectrum. Indeed, propylene oxide which is terminated by a hydroxyl group and a chlorine atom is expected to furnish the 1295, 1353, 1411 Da .... ions.

The polymers have also been examined by electrospray, KIDS, and MALDI. An examination of one specific oligomer allows the identification of C−Cl, C−OH, and =CHR end groups. See Figure 7. Under electrospray conditions we can achieve resolutions in excess of 15 000 which facilitates the comparison between theoretical and experimental isotope distributions to provide support for our molecular formula assignments. Thus, by comparison of the theoretical isotope distribution (resolution = 15 000) and the measured distribution for the mono-chlorinated 15-mer having a molecular formula of $[C_{45}H_{91}ClO_{15}]Na$ (Figure 7b), the chlorine-containing species were assigned. We based our other end group assignments on similar comparisons. Hence, the LD/FTMS data show several ions corresponding to hydroxyl, chloro, and propenyl end groups, which are also visible in the ^1H and ^{13}C NMR spectra (see Experimental Section).

In one experiment, the deuterium-labeled compound $[(O{\sim\sim}CHMe{\sim\sim}O)Al(O^iPr\text{-}d_7)]_2$ was allowed to react with PO (250 equiv) at room temperature. The sample was then examined by GPC/MS in order to estimate the

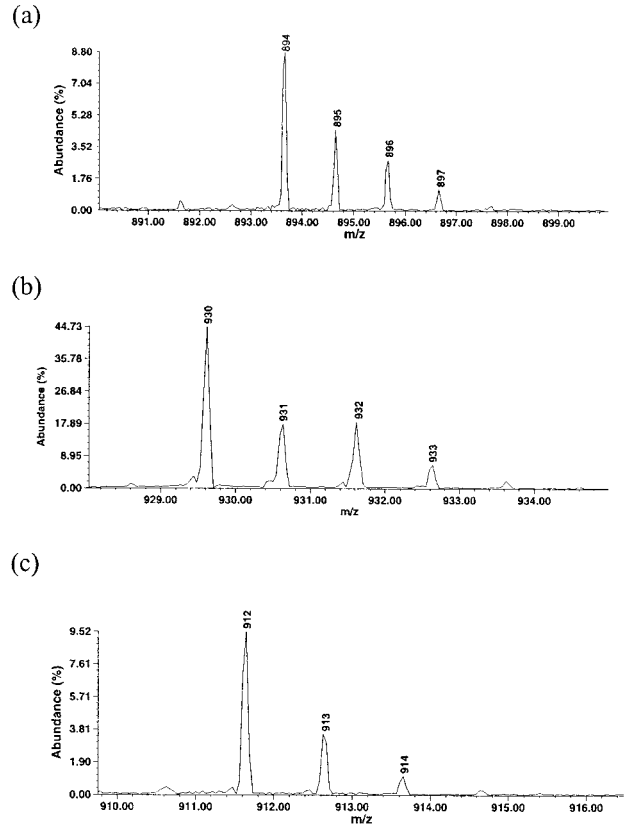

Figure 7. Experimental isotopic distributions for the 15-mer: (a) cyclic or vinyl-terminated $[(C_3H_6O)_{15}]Na^+$, (b) HCl-capped $[Cl-(C_3H_6O)_{15}]Na^+$, and (c) linear $[OH-(C_3H_6O)_{15}]Na^+$.

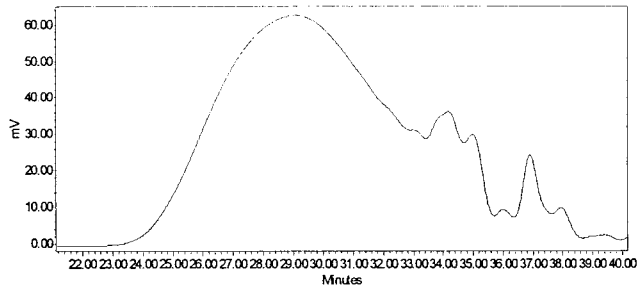

Figure 8. GPC trace for the PPO obtained with the system $[(C_{30}H_{44}O_2)Al(O^iPr\text{-}d_7)]_2$.

percent conversion based on [Al] and in order to examine the influence of an [Al−OR] initiator vs the [Al−Cl] initiators described above. The GPC trace is shown in Figure 8. From this we determine M_n = 1860 Da and M_w = 3180 Da, which gives a PD of 1.7. In contrast to the [Al−Cl]-initiated polymers, the ratio of cycles:linear oligomers is much smaller—though cyclic oligomers are still present. From electrospray data we observed that the majority of the oligomers were $O^iPr\text{-}d_7$ and OH-terminated. In addition, we observed dihydroxy- and hydroxy−vinyl-terminated species. The MS data for the $X-(PO)_{20}-Y$ oligomers obtained with Na^+/electrospray are shown in Figure 9.

By NMR Spectroscopy. ^1H NMR spectroscopy is not in general a very useful tool, but $^{13}C\{^1H\}$ NMR spectroscopy, especially when coupled with various 2D techniques, is. It is useful to present here briefly the prior results of Schilling and Tonelli[22] in conjunction with our studies of the polymerization of PO by (TTP)AlCl and the Union Carbide system.

Simple base polymerization, OH- or OR-induced polymerization, where the countercation is Na^+ or K^+, produces ca. 95% regioregular polymer which Schilling and Tonelli analyzed at triad sensitivity: (HT)(HT)(HT). The $^{13}C\{^1H\}$ spectrum of PPO derived from *rac*-PO and KOH is shown in Figure 10. In the methine carbon region there are three signals assignable to **ii**, **is** + **si**, and **ss**. Polymerization of *S*-PO gives rise to only the **ii** signal. The signal of relative integral intensity 2 is therefore assigned as **is** + **si**. The stereosequences for the (HT)(HT)(HT) triads are shown in **E**. For the

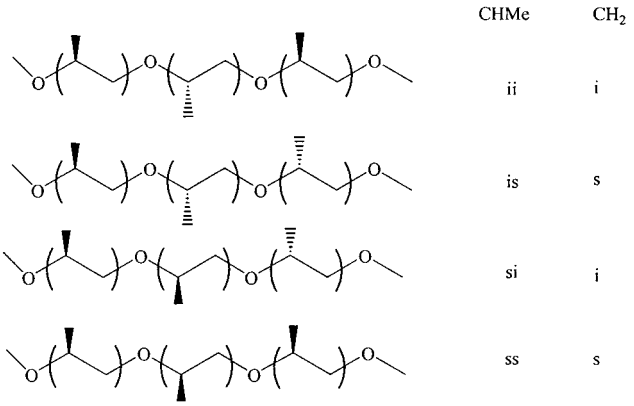

E

(HT)(HT)(HT) triad, there are eight possible stereosequences, but because NMR spectroscopy in a achiral solvent cannot distinguish R and S centers, only the four shown in **E** are detectable; i.e., the **ii** triad for $(S\text{-PO})_3$ is identical to that for $(R\text{-PO})_3$. PPO is an asymmetric polymer and so **is** ≠ **si**. Also, because of this asymmetry, the methylene carbon signals were only assigned at the diad level, namely **i** and **s**, though as can be seen from Figure 10 there is some splitting of the signal assigned to the **s** diad. [We shall return to this point later.]

Polymerization of *rac*-PO by (TPP)AlCl and the Union Carbide system gives a stereoregular $(HT)_n$ polymer, and as shown in Figure 11, there is a preference for isotactic junctions. The **ii** to (**is** + **si**) to **ss** ratio being ca. 50:40:10 for (TTP)AlCl. The preference for isotactic junctions is less pronounced for the Union Carbide catalyst but is still evident. Since (TTP)AlCl is achiral, this must result from end group control in the ring-opening event wherein a Al−O*CHMeCH$_2$−OP stereocenter preferentially ring-opens a molecule of PO of the same chirality. The stereoselectivity is modest especially when compared to the C_2-symmetric $Zn(OMe)_2$·$(Zn(OMe)Et)_6$ cubanes employed by Tsuruta[27] which polymerize *rac*-PO to give isotactic PPO (50:50 -*R*-PPO and *S*-PPO). From an inspection of Figure 11 we can see that the upfield signal of Figure 10 is now clearly resolved into two resonances of unequal intensity. The methylene carbon sensitivity formally assigned to an **s** diad is seen to consist of two signals: an upfield signal which can now be assigned as **ss** and a downfield signal which must therefore be either **is** or **si**. The signal at 74 must then be **ii** + **is** or **ii** + **si**. From the methine carbon intensities we know that **ii** represents 60%, **is** + **si** 40% and **ss** 10% of the total polymer.

In contrast to the regioregular PPO formed by simple base, (TPP)AlCl, and the Union Carbide systems, the aluminum complexes described in this work give highly regioirregular polymers. The ^{13}C NMR spectrum of a PPO sample formed from *rac*-PO and **1** is shown in

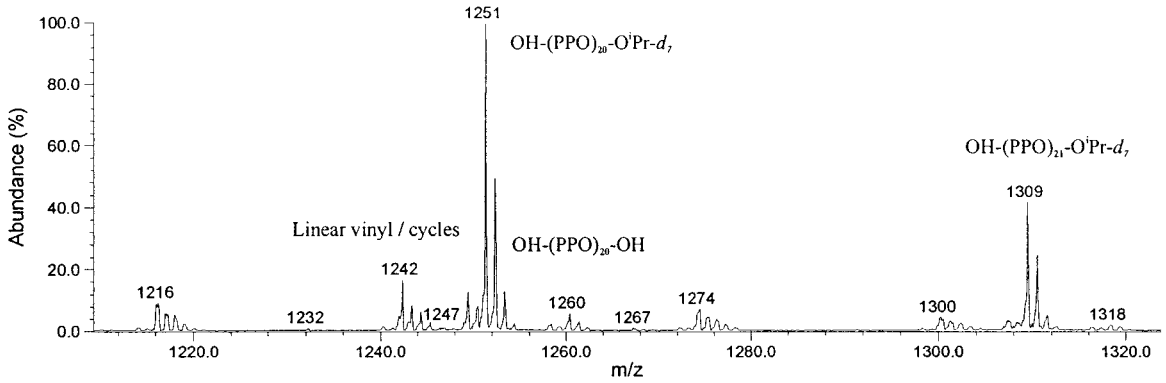

Figure 9. Molecular weight distribution for the X−$(PO)_{20}$−Y oligomers obtained with Na^+/electrospray.

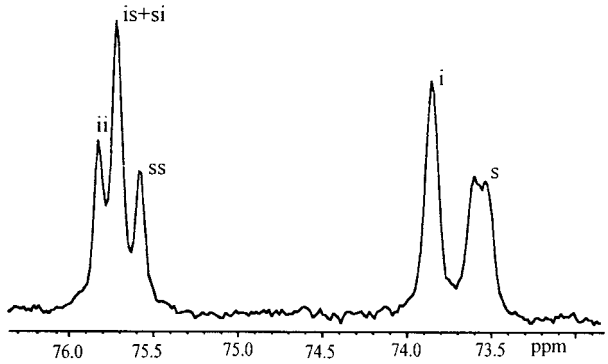

Figure 10. ^{13}C {^1H} NMR showing the methine and methylene carbons of polypropylene oxide obtained from anionic base polymerization.

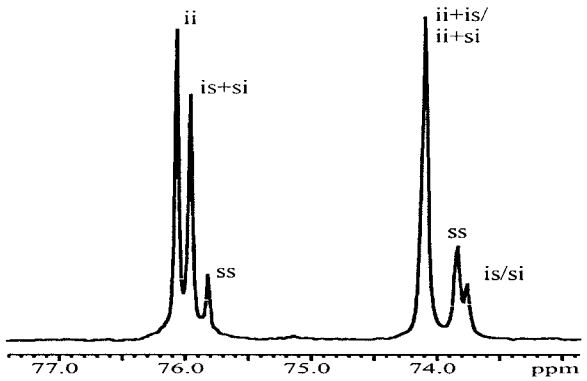

Figure 11. ^{13}C {^1H} NMR spectrum showing the polymer obtained from the reaction of PO with the tetraphenylporphinatoaluminum chloride system.

Figure 12. To distinguish between the methine and methylene carbon ^{13}C signals, we have employed DEPT (distortionless enhancement by polarization transfer) spectroscopy. The DEPT spectra of the same sample of PPO are shown in Figure 13. The sum of the two DEPT spectra in Figure 13 yields the spectrum shown in Figure 12. The most salient feature of the spectra is that the polymer is regioirregular. In addition to the $(HT)_3$ regioregular triads, the regioirregular HH and TH junctions account for roughly 50% of the polymer. The overlap of the HH sequences of the methine carbons with the HT sequences of the methylene carbons and the TT of the methylene with the HT of the methine arises from the γ-effect.[28]

In addition to the ^{13}C signals of PPO, there are ^{13}C signals arising from end groups. These are distinguishable by spin−lattice relaxation time (T_1) measurements, and these are listed in the Supporting Information. Also,

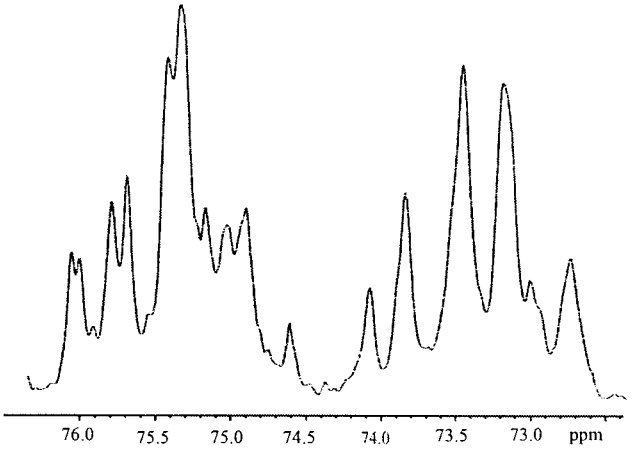

Figure 12. ^{13}C {^1H} NMR of the polymer obtained from *rac*-PO and $[(C_{30}H_{44}O_2)AlCl]_2$ (**1**).

deconvolution experiments were performed to determine the approximate integral intensities of the peaks. These data are also provided in the Supporting Information.

With the intent of elucidating the mechanism of ring opening, we also carried out polymerization of *S*-PO which gave PPO having the DEPT spectra shown in Figure 14 and a 50:50 mixture of *S*-PO:*rac*-PO (i.e., 75% *S*-PO + 25% *R*-PO) which gave a PPO with the ^{13}C DEPT spectra shown in Figure 15. Before we proceed to examine these spectra and the implications they provide with respect to the nature of the ring-opening event, it is necessary to examine the regiosequences for PPO at the triad level and their respective stereosequences.

Microstructural Analysis. At the triad level PPO has eight possible regiosequences as shown in Scheme 2. Each one of these regiosequences has stereochemistry which can lead to the tacticities shown in Figures 16 and 17 for the methine and methylene carbons, respectively. The numbers 1−8 refer to the regiochemistry of the triads for the methine carbons and 9−16 for the methylene carbons. For each regiosequence there are four stereosequences.

Inspection of the methine carbon sequences shown in Figure 16 reveals that the regiosequences 1, 2, 4, and 8 contain a central methine carbon as part of an HT junction while for 3, 5, 6, and 7 the central methine carbon is part of a HH junction. Sequences 1 and 8 are indistinguishable by NMR and represent the regioregular polymer while 2 and 4 are regioirregular with a TT junction. The methine carbons in 1 and 8 will show triad sensitivity but in 2 and 4 only diad sensitivity.

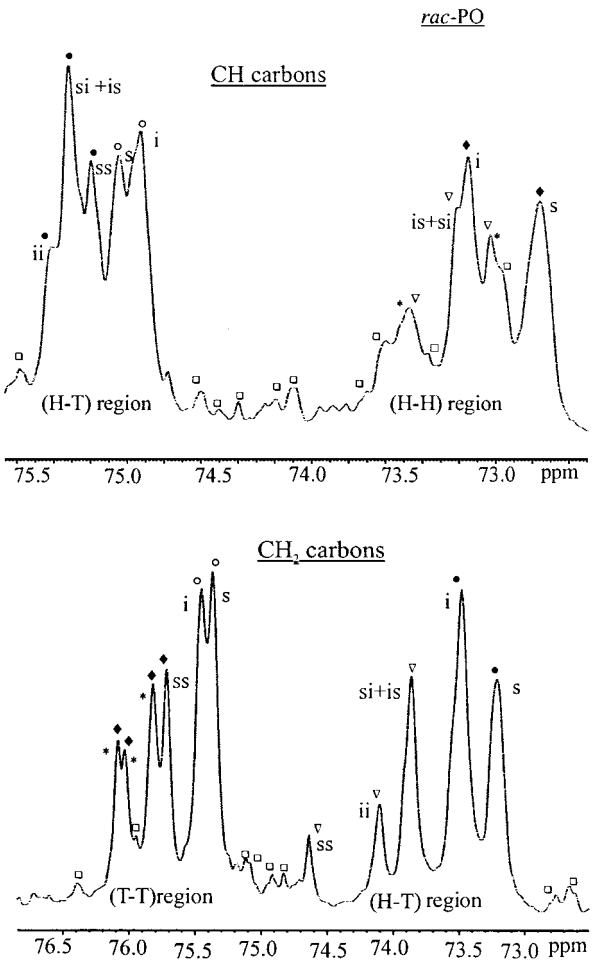

Figure 13. DEPT NMR spectra showing the methine and methylene carbons for the polymer obtained from *rac*-PO and $[(C_{30}H_{44}O_2)AlCl]_2$. Legend: ● (1, 8) and (9, 16), ○ (2, 4) and (10, 12), ♦ (3, 6) and (11, 14), ▽ (5, 7) and (13, 15), □ end groups, * **ii/ss** for ▽ or **is/si/ii** for ♦.

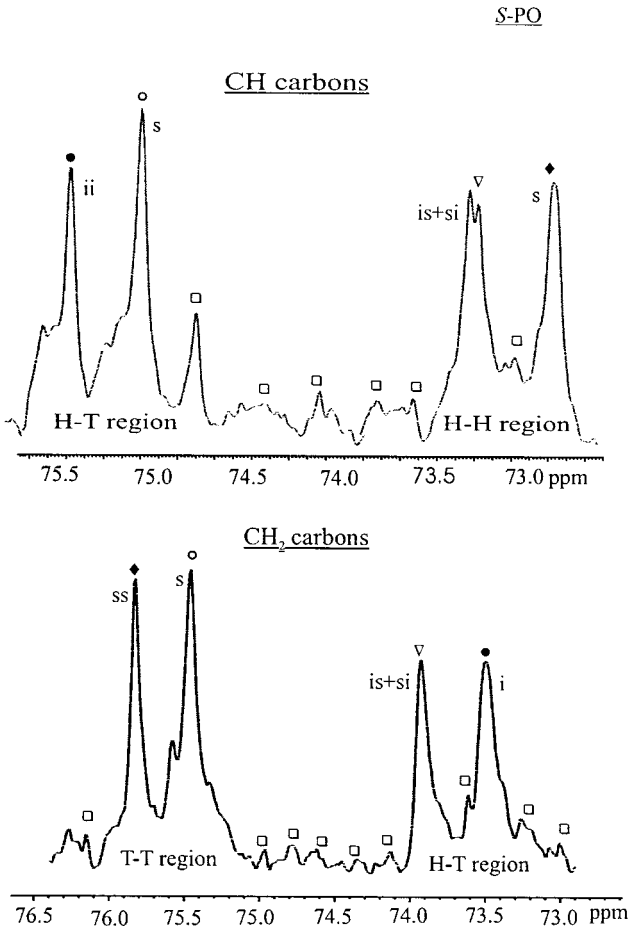

Figure 14. DEPT NMR showing the methine and methylene carbons for the polymer obtained from *S*-PO and $[(C_{30}H_{44}O_2)AlCl]_2$. Legend: ● (1, 8) and (9, 16), ○ (2, 4) and (10, 12), ♦ (3, 6) and (11, 14), ▽ (5, 7) and (13, 15), □ end groups.

The second grouping of methine carbons 3, 5, 6, and 7 all show a HH junction for the central moiety, and in each case there is a methine carbon two bonds removed. For 3 and 6, however, there is only dyad sensitivity while for 5 and 7 there will be triad sensitivity.

Last, it should be recognized that the two groups of regiosequences (1, 2, 4, and 8) and (3, 5, 6, and 7) will be separated in chemical shift by the γ effect. The former with HT junctions will be in the region 75−76 ppm (as seen for stereoregular PPO in Figure 10) while the latter (3, 5, 6, and 7), which have HH junctions, will be upfield at 73−74 ppm. A summary of the regiosequences, the types of connecting units, stereosequences, and ^{13}C NMR chemical shifts is presented in Table 6.

The methylene carbon sequences can be analyzed in an analogous manner. The eight possible regiosequences are labeled 9−16 with 9 and 16 being the regioregular sequence. Because there is one methyl group that is four bonds removed, there is only diad sensitivity, though, as seen in Figures 10 and 11 and previously discussed, some greater resolution is apparent and from the work reported herein allows the assignment of at least **ii** and **ss** for the regioregular sequence (9, 16). Table 7 summarizes the analysis for the methylene carbons and the predictions for the ^{13}C chemical shift regions based on the γ-effect. Recall the assignments for the methine carbons (1 and 8) and methylene carbons (9 and 16) follow from the earlier work of Schilling and Tonelli and are as shown in Figure 10.

We can now proceed to an analysis of the DEPT spectra obtained for PPO from *rac*-PO, *S*-PO, and 50:50 *S*-PO:*rac*-PO. We start with the methine carbons. The first point of note is that polymerization of *S*-PO yields a regioirregular polymer by a stereoselective ring-opening process. The mechanism is not a "simple cationic" mechanism as is seen in the use of BF_3 or $SnCl_4$ as initiators.[29] To go further, we must proceed to examine methine and methylene regions separately and recognize that certain information gleaned from each must be complementary to the other.

The Methine Carbon Spectra. There are five signals in the HT region of the spectrum, 75.0−75.5 ppm. Three are immediately assignable as **ii**, **is**+**si**, and **ss** for the $(HT)_3$ stereoregular triads, sequences 1 and 8. The two others must come from the regio sequences 2 and 4 and may be assigned **i**/**s**. It is not possible to distinguish between **i** and **s** in the polymerization of *rac*-PO. In the ^{13}C spectrum of PPO derived from *S*-PO only the **ii** sequence is present for 1 and 8 and only one of the **i**/**s** signals is present for 2 and 4. A stereoregular HT triad (1, 8) formed from *S*-PO would be **ii** irrespective of the mechanism of ROP (Scheme 1) whereas the HT regioirregular sequences (2 and 4) would be **i** for retention and **s** for backside attack.

In the methine HH region, 72.5−73.5 ppm, which in simple base polymerization accounts for less than 5% of the polymer, we expect to find the stereosequences 5

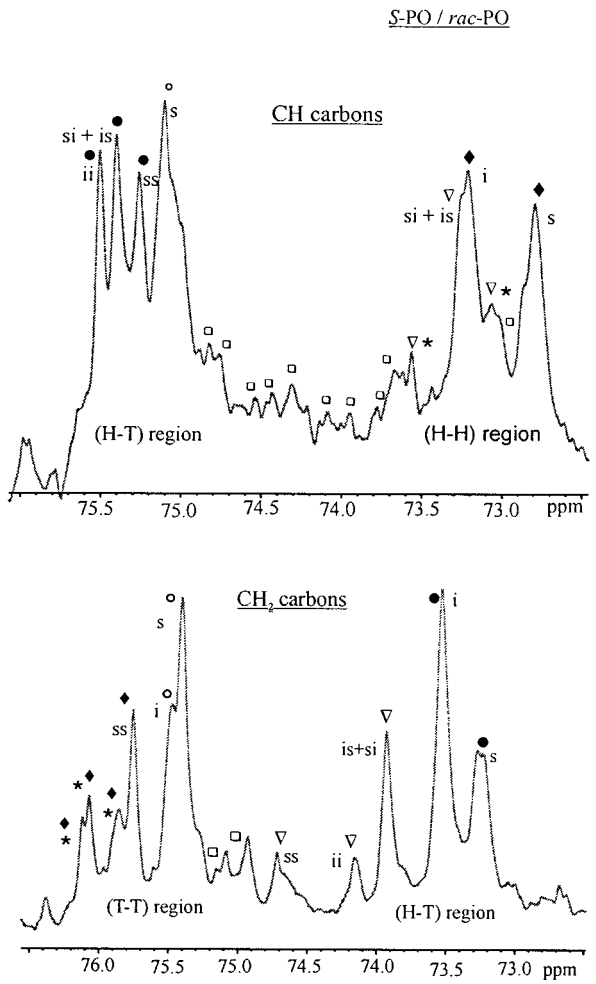

Figure 15. DEPT NMR showing the methine and methylene carbons for the polymer obtained from 50% *rac*-PO and 50% *S*-PO and $[(C_{30}H_{44}O_2)AlCl]_2$. Legend: ● (1, 8) and (9, 16), ○ (2, 4) and (10, 12), ♦ (3, 6) and (11, 14), ▽ (5, 7) and (13, 15), □ end groups, * **ii/ss** for ▽ or **is/si/ii** for ♦.

and 7 and 3 and 6. For *rac*-PO 3 and 6 would give rise to **i** and **s** while 5 and 7 would give rise to **ii**, **is**, **si**, and **ss**. The signals for **i** and **s** from 3 and 6 would be more intense but could not otherwise be distinguished. We have therefore identified the carbon resonance in Figure 13 with ♦ as being derived from 3 and 6 and denoted ▽ for those from 5 and 7. Polymerization of *S*-PO would for 3 and 6 give **s** by inversion and **i** by retention of configuration. The appearance of just one resonance in Figure 14 supports the assignment of 3 and 6 shown in Figure 13 but cannot distinguish between **i** and **s**. However, for the sequence 5 and 7 retention during ROP would yield only **ii** whereas inversion would lead to **is** and **si**. The appearance of two signals at ca. 73.4 ppm thus supports inversion or backside attack. Note the sensitivity is at the triad level. A diad might have yielded ambiguity if sensitivity was higher, thereby revealing a splitting as discussed previously for the **s** diad shown in Figure 10.

In the methylene carbon spectrum of the HT region the regioregular sequences 9 and 16 are readily assigned by comparison with the earlier work of Tonelli and Schilling. For *rac*-PO polymer we would expect 13 and 15 to give **ii**, **is**, **si**, and **ss** stereosequences. Only three other signals (in addition to the **i** and **s** from 9 and 16) are seen so there must be some accidental degeneracy.

Scheme 2. Eight Possible Regiosequences for PO on a Triad Level. Numbers 1−8: Central Methine Carbon Atom. Numbers 9−16: Central Methylene Carbon Atom

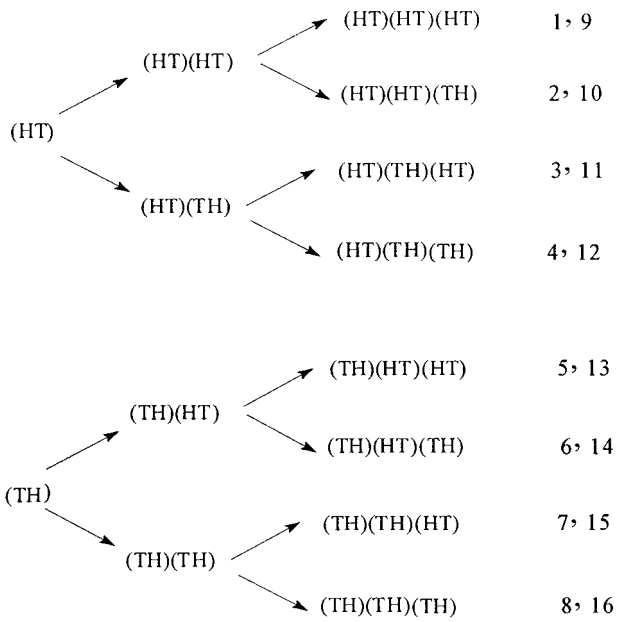

The signals arising from 13 and 15 are noted with a ▽ in Figure 13.

The polymerization of *S*-PO gives **i** for 9 and 16 irrespective of the mechanism of ring-opening. For (13, 15) retention would give **ii** and inversion **is** + **si**. The appearance of a single resonance for (13, 15) is thus ambiguous.

In the TT region of the spectrum, 75.0−76.2 ppm, there are six signals for the poly(*rac*-PO). The stereosequences (10, 12) give rise to **i** and **s** and (11, 14) give rise to **ii**, **is**, **si**, and **ss**. From the relative intensities it seems plausible to assign the upfield signals to the **i**/**s** of (10, 12) and the other signals to (11, 14). For the polymer derived from *S*-PO only two principal signals are seen. For (10, 12) retention would yield **i** and inversion **s** while for (11, 14) retention would yield **ii** and inversion **ss**. The methylene carbon spectra, while complementing the methine carbon spectra, do not prove useful in distinguishing between ROP by retention vs inversion, but the methine spectra do.

Polymerization of 50:50 *rac*:S-PO. The DEPT ^{13}C spectra of PPO formed in the reaction between **1** and a 50:50 mixture of *rac*- and *S*-PO are shown in Figure 15. The spectra are, as would have been expected, the sum of those shown in Figures 13 and 14. A statistical analysis for the sequences 5 and 7 is given in Table 8. Retention of configuration during ROP would yield **ii** being favored over **ss**, **is**, and **si** by the ratio 0.875:0.375:0.375:0.375 while inversion favors **is** and **si**. An inspection of the methine ^{13}C signals is again explained by inversion bearing in mind that the **i** contribution from the 3, 6 stereosequences falls along with the **is** + **si** of 5, 7.

The Biphenoxide Catalyst System. The biphenoxide complexes $[(O\sim\sim O)AlCl]_2$ and $(O\sim\sim O)AlX(THF)$, where X = Cl and Et, are C_2 symmetric, and when these are used to polymerize PO, the resulting PPO shows some stereoselectivity for the ROP process. The DEPT spectra are shown in Figure 18 where it can be seen that for the $(HT)_3$ triad (1, 8 and 9, 16) the stereosequence **ii**:(**is** + **si**):**ss** ratio is approximately 40:60:20.

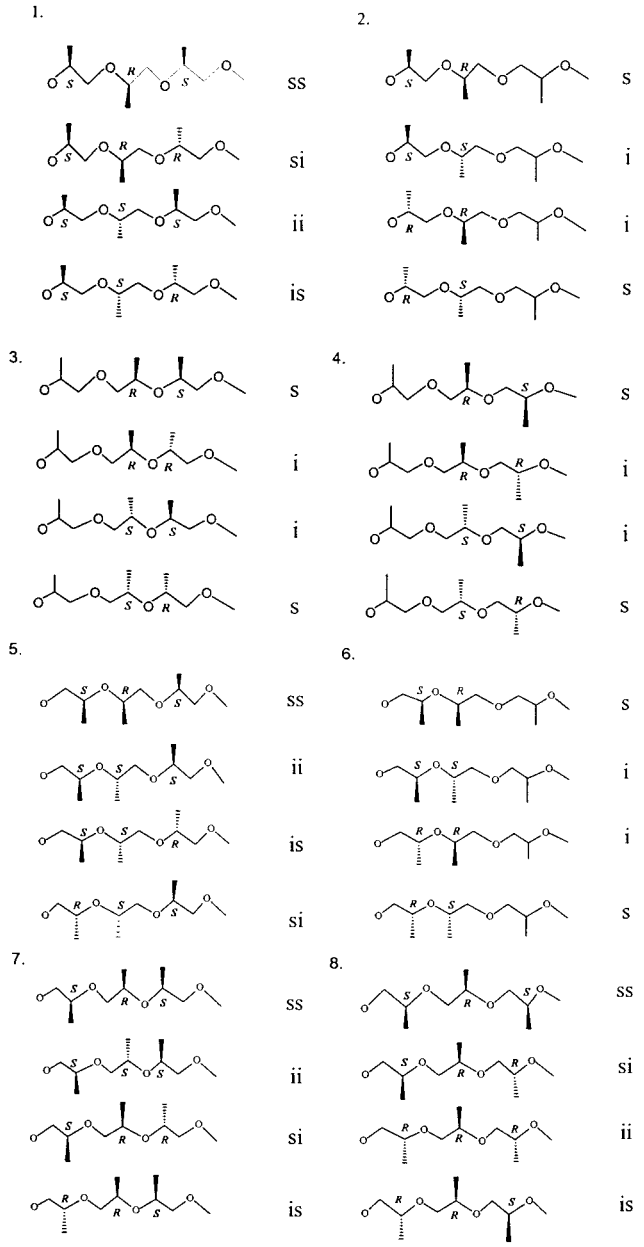

Figure 16. Stereosequences observed when looking at the methine carbon of the central unit. Numbers 1−8 indicate regiosequence. For 2, 3, 4, and 6 the methine carbon is insensitive to the farthest removed stereocenter giving only **i** and **s**.

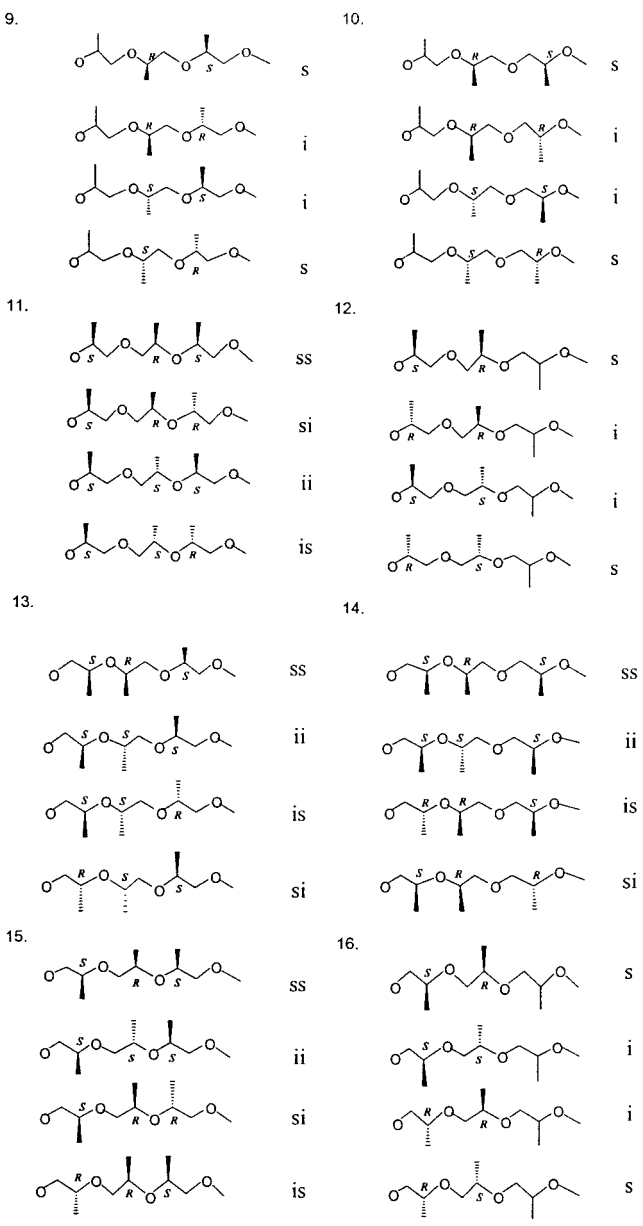

Figure 17. Stereosequences observed when looking at the methylene carbons of the central unit. For 9, 10, 12, and 16 the methine carbon is insensitive to the farthest removed stereocenter giving only **i** and **s**.

Table 6. Summary of ^{13}C Chemical Shifts with Regio- and Stereosequences and Connecting Units for the Methine Carbons of PPO

regio-sequences	connecting units	stereo-sequences	^{13}C NMR (ppm)
1, 8	2 (HT)	ss, is, ii, si	76−75.5
2, 4	1 (HT), 1 (TT)	i, s	75.5−75
5, 7	1 (HT), 1 (HH)	ss, is, ii, si	74−73
3, 6	1 (HH), 1 (TT)	i, s	74−73

Given that we are correct in our assignment of the spectra obtained for the PPO of *S*-PO as shown in Figure 14, we can make further assignments for the stereosequences as shown in Figure 18. The use of the C_2 symmetric Al center imparts some stereoselectivity in the ROP process for HH and TT stereoirregular sequences.

Concluding Remarks

The use of the sterically encumbered biphenols, shown in **B** and **C**, and the substituted binol shown in **D** have allowed the isolation of biphenolate and binolate aluminum chloride complexes that favor cis coordination of Lewis bases such as THF and epoxides. These complexes, together with $[(O{\sim\sim}CHMe{\sim\sim}O)Al(O^iPr\text{-}d_7)]_2$ and $[Cp_2Zr(OEt)(OEt_2)]^+[HB(C_6F_5)_3]^-$, are active in initiating ROP of PO to give PPO which is markedly different in microstructure from that obtained by Inoue's (TPP)AlCl system and the Union Carbide catalyst. The present polymers show a high degree of regioirregularity with ca. 50:50 HT:HH junctions. While this is rather typical of Lewis acid polymerization of PO, the polymerization of *S*-PO by compounds **1**, **2**, **3**, and **4** reveals that the ring-opening event is stereoselective. An analysis of the ^{13}C NMR spectra of PPO derived from *rac*-, *S*- and 50:50 *rac*-, *S*-PO provides evidence for ROP with inversion of stereochemistry at the chiral center. This

Table 7. Summary of ^{13}C Chemical Shifts with Regio- and Stereosequences and Connecting Units for the Methylene Carbons of PPO

regio-sequences	connecting units	stereo-sequences	^{13}C NMR (ppm)
9, 16	2 (HT)	i, s	73−73.6
10, 12	1 (HT), 1 (TT)	i, s	75.2−76.2
13, 15	1 (HT), 1 (HH)	ss, is, ii, si	73.6−74.7
11, 14	1 (HH), 1 (TT)	ss, is, ii, si	75.2−76.2

is not consistent with a cis-migratory ring-opening event.

While we cannot provide unequivocal evidence for the mechanism of polymerization and chain transfer, we can discount a "simple cationic" mechanism of the type observed for HBF_4, BF_3, and $SnCl_4$. The large number of HH and TT junctions is typical of cationic ring-opening polymerization, but the influence of the C_2-symmetric binolate aluminum initiators reveals that some stereoselectivity is imparted by the metal center in the polymerization of *rac*-PO.

The initial ring-opening event follows activation of the PO by coordination to a Al center as in reactions a and b of Scheme 3. As shown, these occur at a single Al center, but we cannot discount that the Cl or OR group from one metal attacks an activated PO coordinated to another. The latter is presumably the operative mechanism for the Inoue and Union Carbide catalyst systems which give stereoregular polymers involving greater than 95% $(HT)_n$ units.

The formation of cyclic oligomers can easily be accounted for by reactions c and e of Scheme 3, for which we would expect reaction c to occur more readily. This is consistent with the greater cyclic:linear oligomers seen in [Al−Cl] initiated polymerization vs that found for [Al−O^{i}Pr-d_7].

The formation of vinyl end groups can be accounted for by dehydrohalogenation from terminal C−Cl groups, reaction d. Dehydration by a reaction f is less likely and vinyl end groups are less prevalent for [Al−O^{i}Pr-d_7] initiated polymerization. Vinyl end groups may also arise from the reaction of a coordinated alkoxide (OP) and propylene oxide to give POH, a hydroxy-terminated oligomer, and allyl alkoxide $CH_2{=}CH{-}CH_2O^-$ which, bound to Al, would then enter into further ring-opening of PO. Any reactions leading to the formation of water, e.g., dehydration of OH-terminated oligomers, would generate AlOH bonds and POH and ultimately loss of catalytic activity. The system is therefore not living. While the fate of the bulk of the aluminum is not known, one compound that can be viewed as a partial hydrolysis product, $[(C_{24}O_2H_{32})_3Al_3(\mu\text{-}O)_3]$, was structurally characterized.[31]

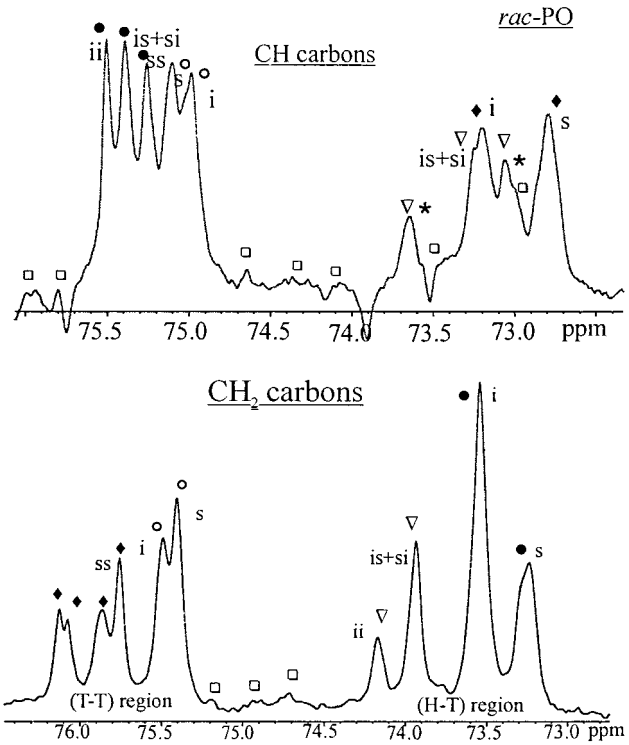

Figure 18. DEPT NMR showing the methine and methylene carbons for the polymer obtained from *rac*-PO and $[(C_{24}H_{32}O_2)$-AlX(THF)] (X = Cl, ethyl). Legend: ● (1, 8) and (9, 16), ○ (2, 4) and (10, 12), ♦ (3, 6) and (11, 14), ▽ (5, 7) and (13, 15), □ end groups, * **ii/ss** for ▽ or **is/si/ii** for ♦.

It is interesting to compare the ring-opening activity of propylene oxide and lactide toward the magnesium, zinc, and aluminum compounds used in the present work and the first paper of this series. These are compared in Table 9. Also included in the table are our findings with the [(BDI)M(OR)(THF)] precursors[32] that are closely related to Coates [(BDI)Zn(O^{i}Pr)]$_2$. None of the monomeric magnesium or zinc precursors are active

Table 8. Statistical Probabilities for the Occurrence of the Triads ii, is + si, and ss for the Regiosequences 5 and 7 from the Polymerization of a 50:50 Mixture of *S*-PO and *rac*-PO (75% *S* + 25% *R*)

inversion for **7**
SSS 0.75 × 0.75 × 0.25 = 0.140625 ii
SSR 0.75 × 0.75 × 0.75 = 0.421875 is
SRR 0.75 × 0.25 × 0.75 = 0.140625 si
RRR 0.25 × 0.25 × 0.75 = 0.046875 ii
RRS 0.25 × 0.25 × 0.25 = 0.015625 is
SRS 0.75 × 0.25 × 0.25 = 0.046875 ss
RSS 0.25 × 0.75 × 0.25 = 0.046875 si
RSR 0.25 × 0.75 × 0.75 = 0.140625 ss

retention for **7**
SSS 0.75 × 0.75 × 0.75 = 0.421875 ii
SSR 0.75 × 0.75 × 0.25 = 0.140625 is
SRR 0.75 × 0.25 × 0.25 = 0.046875 si
RRR 0.25 × 0.25 × 0.25 = 0.015625 ii
RRS 0.25 × 0.25 × 0.75 = 0.046875 is
SRS 0.75 × 0.25 × 0.75 = 0.140625 ss
RSS 0.25 × 0.75 × 0.75 = 0.140625 si
RSR 0.25 × 0.75 × 0.25 = 0.046875 ss

inversion for **5**
SSS 0.75 × 0.25 × 0.25 = 0.046875 ii
SSR 0.75 × 0.25 × 0.75 = 0.140625 is
SRR 0.75 × 0.75 × 0.75 = 0.421875 si
RRR 0.25 × 0.75 × 0.75 = 0.140625 ii
RRS 0.25 × 0.75 × 0.25 = 0.046875 is
SRS 0.75 × 0.75 × 0.25 = 0.140625 ss
RSS 0.25 × 0.25 × 0.25 = 0.015625 si
RSR 0.25 × 0.25 × 0.75 = 0.046875 ss

retention for **5**
SSS 0.75 × 0.75 × 0.75 = 0.421875 ii
SSR 0.75 × 0.75 × 0.25 = 0.140625 is
SRR 0.75 × 0.25 × 0.25 = 0.046875 si
RRR 0.25 × 0.25 × 0.25 = 0.015625 ii
RRS 0.25 × 0.25 × 0.75 = 0.046875 is
SRS 0.75 × 0.25 × 0.75 = 0.140625 ss
RSS 0.25 × 0.75 × 0.75 = 0.140625 si
RSR 0.25 × 0.75 × 0.25 = 0.046875 ss

total inversion for **5** and **7**
ii = 0.375, is = si = 0.625 ss = 0.375

total retention for **5** and **7**
ii = 0.8750, is = si = ss = 0.375

Scheme 3. Proposed Reactions Leading to the Different End Groups Observed in the GPC/MS Spectrum of the Polymer PPO Formed with the System [(O∼CHMe∼O)AlX]$_2$, X = Cl, ^{i}PrO-d_7

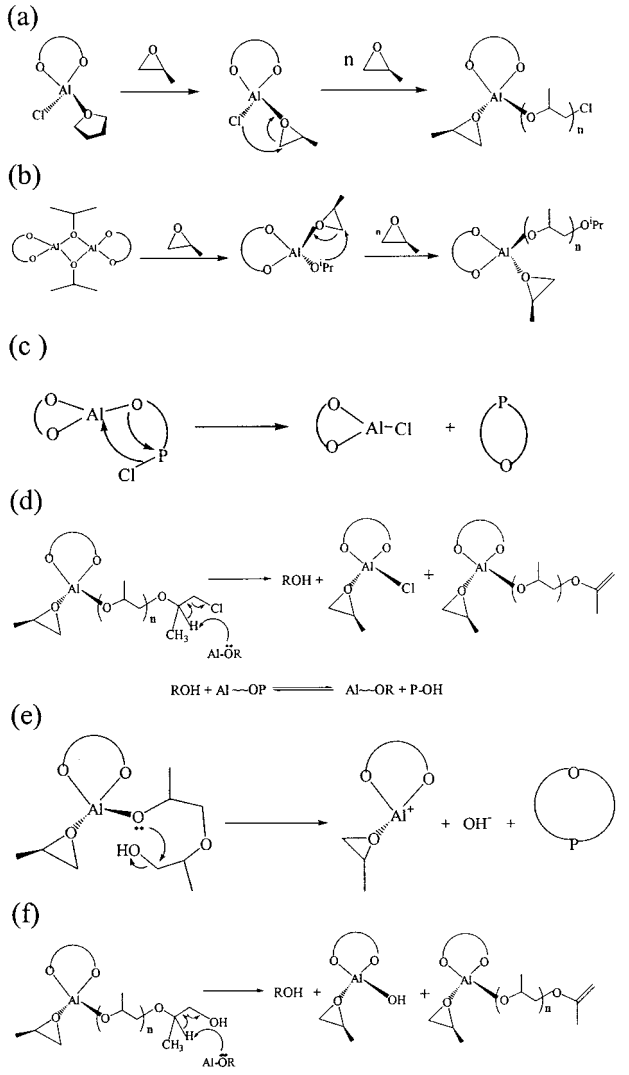

Table 9. Comparison of the Activity of Various Catalyst Precursors in the Ring-Opening Polymerization of PO and Lactide at 25 °C

catalyst precursor	active	inactive
[(O∼∼O)AlCl]$_2$	PO	lactide
TPPAlCl	PO	lactide
[(O∼∼O)AlOR]$_2$	PO	lactide[a]
TPPAlOR	PO	lactide[b]
(Tp)MOR	lactide	PO
[(BDI)ZnO^{i}Pr]$_2$	lactide	PO
[(BDI)MgOR(THF)]	lactide	PO

[a] Lactide polymerization is observed in benzene at 80 °C. [b] Lactide polymerization is very slow even at 100 °C in benzene.

for ROP of PO, yet each is active for ROP of lactide. The aluminum chloride complexes will initiate ring opening of PO but not lactides. The aluminum alkoxide complexes of the form [(O∼∼O)Al(OR)]$_2$ and [(O∼∼O)-Al(OR)(THF)] will polymerize both lactide and PO (but not in a living manner). Lactide polymerization in benzene only occurs upon heating—quite probably because the dimeric alkoxide-bridged structure is present at lower temperatures.

It seems likely that the reason for the inactivity of the tris(pyrazolylborate)magnesium and -zinc alkoxide complexes of formula TpMOR (Tp = a tris(pyrazolylborate))[1] and [(BDI)M(OR)(THF)] complexes to initiate ROP of PO is due to the inability of the cis-migratory mechanism to operate and the inability of a bimolecular mechanism involving backside attack to take over, perhaps as a result of steric constraints. The same would seem to be true for the [(BDI)Zn(O^{i}Pr)]$_2$ catalyst system of Coates[30] which is active in the stereoselective polymerization of *rac*-lactide. If these present findings can be generalized, then the future design of well-defined coordinate catalysts for ROP of PO should focus on dinuclear or polynuclear metal complexes where two metal centers can act in a cooperative manner, whereas lactide polymerization can be achieved by single metal-site catalyst systems. This conclusion is consistent with the work of Tsuruta,[27] who found that discrete zinc alkoxide cluster precursor complexes such as [Zn(OMe)$_2$]-[(Et)Zn(OMe)]$_6$ could polymerize *rac*-PO to give stereoregular (HTHTHT) isotactic PPO.

Experimental Section

All syntheses were done under an argon atmosphere using standard Schlenk line and drybox techniques. Solvents were distilled from sodium benzophenone ketyl under nitrogen. Propylene oxide was stirred over calcium hydride for 24 h and distilled under nitrogen. Diethylaluminum chloride, diethylaluminum ethoxide, ethylidenebis(4,6-di-*tert*-butylphenol), 2,2′-methylidene bis(6-di-*tert*-butyl-4-dimethylphenol), and 5,10,15,20-tetraphenylporphine were purchased from Aldrich and used as received. The ligand racemic 5,5′,6,6′-tetramethyl-3,3′-di-*tert*-butyl-1,1′-biphen-2,2′-diol (BiphenH$_2$, Strem) was sublimed prior to use. Potassium hydroxide was dried in a vacuum oven prior to use at 180 °C. BF_3 etherate (Fluka) was used as purchased.

NMR Experiments. NMR experiments were carried out with a ^{UNITY}INOVA spectrometer operating at proton Lamor frequency of 400 MHz and a Varian Gemini 2000 spectrometer operating at 300 MHz proton Lamor frequency. ^{1}H NMR, ^{13}C NMR, distortionless enhancement by polarization transfer (DEPT), and 1D nuclear Overhauser difference spectroscopy (nOe) experiments were performed. In these experiments, ^{13}C coupling constant values of 130 Hz and d1 times of 5 s were used. ^{13}C spin−lattice relaxation times (T_1) were mesured with the standard 180°−τ−90° inversion−recovery sequence. Their peak frequencies were referenced against the respective solvents, benzene-d_6 at 7.15 ppm, toluene-d_8 at 2.05 ppm, and tetrahydrofuran-d_8 at 1.73 ppm. The deconvolution of ^{13}C NMR and DEPT was done using Felix 95 and Vnmr 6.2 Varian software.

Synthesis of 2,2′-Ethylidenebis(4,6-di-tert-butylphenoxide)-aluminum Chloride Dimer, [(C$_{30}$H$_{44}$O$_2$)AlCl]$_2$. Et$_2$AlCl (1 M solution in hexanes, 4 mL, 4 mmol) was placed in a flask containing 15 mL of hexanes. This solution was added via cannula at −10 °C to an equimolar solution of 2,2′-ethylidenebis(4,6-di-*tert*-butylphenol) (1.755 g) in 30 mL of toluene. The mixture was warmed to room temperature and was left stirring for 4 h. The solvent was evaporated under vacuum, and the resulting white powder was washed with hexane (3 × 20 mL). A white solid was obtained. Yield 1.8 g (90%). Recrystallization was done from toluene at −20 °C to give crystals for X-ray diffraction.

IR (Nujol, cm^{-1}): 2957 (s), 1464 (w), 1200 (s), 1100 (s), 950 (s), 800 (s). ^{1}H NMR (toluene-d_8, δ, ppm): 1.05 (s, ^{t}Bu), 1.35 (s, ^{t}Bu), 1.42 (s, ^{t}ubs), 1.47 (s, ^{t}Bu), 2.10 (d, CH$_3$), 5.04 (q, CH), 7.27, 7.43, 7.44, 7.73 (aromatic).^{13}C NMR (toluene-d_8, δ, ppm): 22.57 (s, Me), 30.69 (s, ^{t}Bu), 31.07 (s, ^{t}Bu), 32.11 (s, ^{t}Bu), 33.15 (s, ^{t}Bu), 34.03 (s, *C*(CH$_3$)$_3$), 34.69 (s, *C*(CH$_3$)$_3$), 34.90 (s, *C*(CH$_3$)$_3$), 35.38 (s, *C*(CH$_3$)$_3$), 36.48 (CH), 120.77, 122.79, 125.43, 125.79, 134.25, 138.13, 138.35, 140.54, 142.43, 143.35, 148.95, 150.24 (aromatic). EA: Calcd: C, 72.19; H, 8.88. Found: C, 72.76; H, 9.05%.

Synthesis of 2,2′-Ethylidenebis(4,6-di-tert-butylphenoxide)-aluminum Chloride Tetrahydrofuran Adduct, [(C$_{30}$H$_{44}$O$_2$)AlCl-

(THF)]. The dimer was dissolved in the minimum amount of THF at room temperature and left to recrystallize at −30 °C. After 1 week, white crystals suitable for X-ray diffraction were obtained.

^{1}H NMR (THF-d_8, δ, ppm): 1.15 (s, THF), 1.40 (s, ^{t}Bu), 1.63 (s, ^{t}Bu), 1.76 (d, CH_3), 3.68 (s, THF), 4.65 (q, CH), 7.40 (aromatic), 7.69 (aromatic). ^{13}C NMR (THF-d_8, δ, ppm): 22.84 (s, Me), 25.49 (q, THF), 30.63 (s, CH), 31.16, 32.11 (s, ^{t}Bu), 35.00, 35.81 ($C(CH_3)_3$), 64.40 (q, THF), 121.49, 121.77, 135.06, 137.06, 137.62, 140.84, 152.9 (aromatic).

Synthesis of 2,2′-Methylidenebis(4-di-methyl-6-di-tert-butylphenoxide)aluminum Chloride Dimer, [($C_{23}H_{30}O_2$)AlCl]$_2$. Et_2AlCl (1 M solution in hexanes, 4 mL, 4 mmol) was placed in a flask containing 15 mL of hexanes. This solution was added via cannula at −10 °C to an equimolar solution of 2,2′-methylidenebis(4-dimethyl-6-di-*tert*-butylphenol) (1.362 g) in 30 mL of toluene. The mixture was warmed to room temperature and was left stirring for 4 h. The solvent was evaporated, and the resulting white powder was washed with hexane (3 × 20 mL). Yield 1.28 g (80%). Because of solubility problems with hydrocarbon solvents, the product was dissolved in THF-d_8 for further characterization.

IR (Nujol, cm^{-1}): 3000 (s), 1772 (w), 1450 (w), 1278 (s), 1100 (s) 920 (s), 700 (s), 530 (s).

^{1}H NMR (THF-d_8, δ, ppm): 1.37 (s, ^{t}Bu), 1.75 (s, THF), 2.17 (s, CH_3), 3.30 (d, CH_2), 3.58 (s, THF), 4.11 (d, CH_2), 6.9, 7.0 (aromatic). ^{13}C NMR (THF-d_8, δ, ppm): 21.14 (s, Me), 25.38 (THF), 30.65 (s, ^{t}Bu), 33.63 (s, CH_2), 35.50 (s, $C(CH_3)_3$), 67.4 (THF), 126.09, 127.18, 129.65, 131.13, 138.42, 153.65 (aromatic). EA: Calcd: C, 68.90; H, 7.54. Found: C, 68.89; H, 7.99%.

Synthesis of Racemic (5,5′,6,6′-Tetramethyl-3,3′-di-tert-butyl-1,1′-biphen-2,2′-diolate)aluminum Chloride−Ethyl Tetrahydrofuran Adduct, [($C_{24}O_2H_{32}$)AlCl$_{0.2}$(CH_2CH_3)$_{0.8}$THF]. The ligand racemic 5,5′,6,6′-tetramethyl-3,3′-di-*tert*-butyl-1,1′-biphen-2,2′-diol (BiphenH_2) (1.416 g, 4 mmol) was dissolved in THF (30 mL). A solution of Et_2AlCl (1 M solution in hexanes, 4 mL, 4 mmol) in 10 mL of hexanes was slowly added to the ligand at −30 °C. The resulting solution was stirred overnight, and the solvents, THF, and hexanes were evaporated under vacuum. The solid obtained was washed with cold hexanes (3 × 30 mL) and filtered. A white-yellowish powder was obtained. Yield: 30%.

IR (KBr, cm^{-1}): 2950 (s), 1480 (s), 1425 (s), 1265 (s), 1034 (s), 996 (s), 706 (s), 597 (s).

^{1}H NMR (C_6D_6, δ, ppm): 0.05 (m, C*H*HCH$_3$), 0.21 (m, CH*H*CH$_3$), 1.10 (s, THF), 1.20 (t, CH_2CH_3), 1.63, 1.64 (d, ^{t}Bu), 1.75, 1.80 (d, CH_3), 2.14, 2.19 (d, CH_3), 3.34 (s, THF), 7.18, 7.21 (aromatic). ^{13}C NMR (C_6D_6, δ, ppm): 9.50 (CH_2CH_3), 16.95, 17.05 (d, CH_3), 20.50, 20.54 (d, CH_3), 24.61 (s, THF), 29.83 (CH_2CH_3), 30.86, 30.95 (d, ^{t}Bu), 35.06 (s, $C(CH_3)_3$), 73.40 (s, THF), 126.04, 126.93, 127.18, 127.38, 130.68, 131.20, 135.13, 135.32, 135.72, 136.31, 153.83, 155.12 (aromatic). EA: Calcd: C, 74.96; H, 9.44. Found: C, 68.72; H, 8.79%.

The product was dissolved in hot toluene and placed in a NMR tube. Slow evaporation of the solvent under an argon atmosphere gave crystals suitable for X-ray diffraction analysis.

Synthesis of Racemic (5,5′,6,6′-Tetramethyl-3,3′-di-tert-butyl-1,1′-biphen-2,2′-diolate)aluminum Chloride Tetrahydrofuran Adduct, [($C_{24}O_2H_{32}$)AlCl(THF)]. The ligand racemic 5,5′,6,6′-tetramethyl-3,3′-di-*tert*-butyl-1,1′-biphen-2,2′-diol (BiphenH_2) (1.416 g, 4 mmol) was dissolved in THF (30 mL). A solution of Et_2AlCl (1 M solution in hexanes, 4 mL, 4 mmol) in 10 mL of hexanes was slowly added to the ligand at −30 °C. The resulting solution was heated under reflux at 85 °C overnight. The solvents were evaporated under vacuum. The solid obtained was washed with hexanes (3 × 30 mL) and filtered. A white powder was obtained. Yield: 60%.

^{1}H NMR (toluene-d_8, δ, ppm): 0.91 (s, THF), 1.65 (s, ^{t}Bu), 1.78 (s, CH_3), 2.09 (q, toluene-d_8), 2.19 (s, CH_3), 3.49 (s, THF), 7.21 (s, aromatic). ^{13}C NMR (toluene-d_8, δ, ppm): 16.85, (s, CH_3), 20.39 (s, CH_3), 20.41 (q, toluene-d_8), 24.82 (s, THF), 30.99 (s, ^{t}Bu), 35.02 (s, $C(CH_3)_3$), 73.61 (s, THF), 125.12 (t, toluene-d_8), 127.12 (aromatic), 127.34 (aromatic), 127.96, 128.86 (toluene-d_8), 130.71, 135.27, 136.35, 137.5 (toluene-d_8), 153.89 (aromatic). EA: Calcd: C, 69.05; H, 8.28; Cl, 7.28. Found: C, 63.94; H, 8.29; Cl, 7.61%.

Synthesis of Racemic (5,5′,6,6′-Tetramethyl-3,3′-di-tert-butyl-1,1′-biphen-2,2′-diolate)aluminum Chloride Dimer, [($C_{24}O_2H_{32}$)-AlCl]$_2$. The ligand racemic 5,5′,6,6′-tetramethyl-3,3′-di-*tert*-butyl-1,1′-biphen-2,2′-diol (BiphenH_2) (1.416 g, 4 mmol) was dissolved in hexanes (30 mL). A solution of Et_2AlCl (1 M solution in hexanes, 4 mL, 4 mol) in 10 mL of hexanes was added to the ligand, slowly at −30 °C. Upon addition of the solution of Et_2AlCl/hexanes the solution turned orange immediately. The reaction mixture was warmed to room temperature. After 4 h, a white precipitate formed which was filtered from an orange solution. The white solid was washed with hexanes (3 × 30 mL). The excess solvent was evaporated under vacuum to give a white solid. Yield: 65%. EA: Calcd: C, 69.47; H, 7.77; Cl, 8.54; O, 7.71. Found: C, 64.86; H, 7.95; Cl, 8.48; O, 7.59%.

The product was dissolved in hot benzene and placed in a NMR tube. Slow evaporation of the solvent under an argon atmosphere gave crystals suitable for X-ray diffraction analysis. The product was found to be insoluble in most common hydrocarbon and chlorinated solvents. Upon addition of THF, the product dissolved quickly to give the monomeric tetrahydrofuran adduct.

^{1}H NMR (THF-d_8, δ, ppm): 1.42 (s, ^{t}Bu), 1.62 (s, CH_3), 2.15 (s, CH_3), 3.58 (s, THF), 6.98 (s, aromatic). ^{13}C NMR (THF-d_8, δ, ppm): 16.73, (s, CH_3), 20.36 (s, CH_3), 25.30 (q, THF), 30.94 (s, C(CH_3)$_3$), 35.28 (s, $C(CH_3)_3$), 67.40 (q, THF), 127.37, 127.41, 131.21, 135.13, 137.09, 154.50 (aromatic).

Synthesis of Racemic (5,5′,6,6′-Tetramethyl-3,3′-di-tert-butyl-1,1′-biphen-2,2′-diolate)aluminum Ethyl Tethahydrofuran Adduct, [($C_{24}O_2H_{32}$)Al(CH_2CH_3)(THF)]. The racemic 5,5′,6,6′-tetramethyl-3,3′-di-*tert*-butyl-1,1′-biphen-2,2′-diol (BiphenH_2) (1.416 g, 4 mmol) was dissolved in THF (30 mL). A solution of Et_2AlOEt (1.6 M solution in toluene, 2.5 mL, 4 mmol) in 10 mL of toluene was added to the diol, slowly at −30 °C. The resulting solution was heated at 65 °C overnight. The volatile compounds were evaporated under vacuum. The solid obtained was washed with cold hexanes (3 × 30 mL, product partially soluble) and filtered. The product was dried under vacuum, and a white powder was obtained. Yield: 20%.

^{1}H NMR (toluene-d_8, δ, ppm): 0.05 (m, C*H*HCH$_3$), 0.18 (m, CH*H*CH$_3$), 0.91 (s, THF), 1.21 (t, CH_2CH_3), 1.64 (s, ^{t}Bu), 1.80 (s, CH_3), 2.09 (q, toluene-d_8), 2.21 (s, CH_3), 3.34 (s, THF), 7.19 (s, aromatic). ^{13}C NMR (toluene-d_8, δ, ppm): 8.88 (s, ethyl), 16.93, (s, CH_3), 20.39 (s, CH_3), 20.41 (q, toluene-d_8), 24.71 (s, THF), 29.77 (s, ethyl), 30.82 (s, ^{t}Bu), 35.02 (s, $C(CH_3)_3$), 72.33 (s, THF), 125.12 (t, toluene-d_8), 125.93 (aromatic), 126.86 (aromatic), 127.94, 128.83 (toluene-d_8), 131.21, 135.05, 135.66, 137.46 (toluene-d_8), 155.11 (aromatic). EA: Calcd: C, 74.96; O, 9.99; H, 9.44. Found: C, 72.37; O, 8.81; H, 9.33%.

Synthesis of 2,2′-Ethylidenebis(4,6-di-tert-butylphenoxide)-aluminum Methyl Dimer, [($C_{30}H_{44}O_2$)AlMe]$_2$. Me_3Al (2 M solution in hexanes, 6.83 mmol, 3.41 mL) was placed in a flask containing 10 mL of hexanes. This solution was added via cannula at −10 °C to an equimolar solution of 2, 2′-ethylidenebis(4,6-di-*tert*-butylphenol) (3.0 g) in 30 mL of toluene. The mixture was warmed to room temperature and was left stirring for 4 h, after which time a white precipitate formed. The solvent was evaporated under vacuum, and the resulting white powder was washed with hexane (3 × 20 mL). Yield: 1.6 g (50%).

IR (KBr, cm^{-1}): 2974 (s), 1477 (m), 1204 (s), 1099 (s), 946 (m), 820 (s), 648 (s), 540 (m).

^{1}H NMR ($CDCl_3$, ppm): −0.27 (s, CH_3), 1.23, 1.26, 1.34, 1.43 (s, ^{t}Bu), 1.72 (d, CHC*H*$_3$), 4.73 (q, C*H*CH$_3$), 7.10, 7.21, 7.40 (aromatic).^{13}C NMR ($CDCl_3$, ppm): 22.2 (s, CH_3), 30.3 (s, CH_3), 30.6, 31.2, 41.8, 32.8 (s, C(CH_3)$_3$), 32.5 (s, CH), 34.4, 34.5, 34.9, 36.0 (s, $C(CH_3)_3$), 119.9, 121.6, 124.0, 124.4, 133.9, 136.6, 138.1, 139.9, 140.3, 143.4, 146.9, 150.8 (aromatic).

Synthesis of 2,2′-Ethylidenebis(4, 6-di-tert-butylphenoxide)-aluminum Isopropoxide Dimer, [($C_{30}H_{44}O_2$)Al(O^iPr-d_7)]$_2$ (according to Ko, B. J.; Wu, C. C.; Lin, C. C. *Organometallics* **2000**, *19*, 1864−1869). The dimer [($C_{30}H_{44}O_2$)AlCH_3]$_2$ (0.7 g,

Table 10

catalyst:monomer	catalyst (mmol)	compd **1** (g)	compd **2** (g)
1:500	0.14	0.143	0.114
1:1000	0.07	0.071	0.057
1:5000	0.014	0.014	0.011

0.73 mmol) was dissolved in 30 mL of toluene. An excess of 2-propanol-d_8 (1.46 mmol, 112 μL) was added at room temperature to this solution. The mixture was left stirring overnight at room temperature. A white solid was obtained after recrystallization from hot toluene. Yield: 0.8 g (71%).

IR (KBr, cm^{-1}): 2958 (s), 2869 (s), 2232 (m, C−D stretch), 1476 (s), 1443 (s), 1272 (m), 1239 (s), 970 (s), 879 (m). ^{1}H NMR ($CDCl_3$, ppm): 1.30 (s, C(CH_3)$_3$), 1.38 (s, C(CH_3)$_3$), 1.58 (d, OCH(CH_3)$_2$), 1.80 (d, CHCH_3), 4.21 (q, CHCH$_3$), 4.60 (m, (OCH(CH$_3$)$_2$), 7.16, 7.39 (d, aromatic). ^{13}C NMR ($CDCl_3$, ppm): 22.5 (CHCH_3), 24.8 (OCH(CH_3)$_2$), 33.1 ($CHCH_3$), 30.2, 31.6, 34.3, 35.3 (*tert*-butyl), 71.6 (OCH(CH$_3$)$_2$), 121.0, 121.8, 132.5, 137.1, 140.9, 150.8 (aromatic).

Synthesis of (5,10,15,20-Tetraphenylporphinato)aluminum Chloride, [TPPAlCl] (according to ref 11). To a solution of the porphyrin 5,10,15,20-tetraphenylporphine [(TPP)H$_2$] (0.61 g, 1.2 mmol) in 30 mL of chloroform was added a solution of diethylaluminum chloride (Et$_2$AlCl 1 M solution in hexanes, 1.2 mmol, 1.2 mL) diluted in 10 mL of hexanes. The addition was done slowly at room temperature. The resulting solution was left stirring 3 h after which the solvent was removed under vacuum to give a purple powder. Yield: 80%.

^{1}H NMR (C_6D_6, δ, ppm): 7.4, 8.0, 9.1 (aromatic). ^{13}C NMR (C_6D_6, δ, ppm): 148.5, 141.1, 134.2, 132.4, 128.1 (aromatic), 126.9 (s, CH), 120.7 (s, CH).

Synthesis of Calcium Amide−Alkoxide Catalyst, [(PrO)-$CaNH_2$]$_n$ (modification from procedure described by Goeke, G. L.; et al.; ref 20). Ammonia (10 mL) was condensed at −40 °C into a flask containing calcium (dendritic, 250 mg, 6.2 mmol). A deep blue solution was formed as calcium was dissolved. To this solution was added a mixture of acetonitrile (130 μL, 2.5 mmol) and propylene oxide (250 μL, 3.7 mmol) by syringe at −40 °C. A white precipitate formed immediately. After stirring at −40 °C for 15 min, ammonia was allowed to evaporate by warming the solution slowly to 0 °C under an argon purge. The white solid was dried under vacuum for 1 h at 100 °C and for 3 h at 200 °C, after which time 250 mg of a pale yellow solid was obtained.

Polymerization Reactions. Polymerization reactions were done under an inert atmosphere either in the glovebox or by using Schlenk line techniques. All polymerizations were performed in bulk at room temperature, unless otherwise indicated. Conditions of polymerization varied according to the initiator used (see below). All polymers obtained were characterized by ^{1}H, ^{13}C{^{1}H}, and/or DEPT NMR spectroscopy. The pertinent NMR data are reported in each case. When available, MS data are also reported. For the catalyst precursors presented in this work, such as [($C_{30}H_{44}O_2$)AlCl]$_2$, [($C_{24}O_2H_{32}$)-AlX(THF)], (X = Cl, ethyl), and [($C_{30}H_{44}O_2$)AlO^iPr]$_2$, the percent conversion was calculated on the basis of the weight difference once the excess PO monomer had been removed under vacuum. For all the catalytic systems mentioned above, typical values for conversion at 48 h were between 40 and 50%. For the system [($C_{30}H_{44}O_2$)AlCl]$_2$ (0.014 g, 0.014 mmol) dissolved in 300 μL of PO (4.28 mmol), with a monomer-to-catalyst ratio of 300:1, the conversion was 54% at 48 h. For the system [($C_{24}O_2H_{32}$)AlCl]$_2$ (0.014 g, 0.017 mmol) dissolved in 300 μL of PO (4.28 mmol), with a monomer-to-catalyst ratio of 250:1, the conversion was 41% at 48 h.

rac-PO/[($C_{30}H_{44}O_2$)AlCl]$_2$. The catalyst was taken in a vial, and 5 mL of propylene oxide was added under nitrogen. The different ratios of catalyst:monomer are seen in Table 10. The mixture was stirred at room temperature under nitrogen for 48 h, after which any excess propylene oxide and volatile oligomers were removed under vacuum.

DEPT NMR (C_6D_6, δ, ppm, (tacticity, regiosequence)): CH carbons, H−T region: 75.39 (**ii**, (1, 8)), 75.30 (**si** + **is**, (1, 8)), 75.18 (**ss**, (1, 8)), 75.03 (**s**, (2, 4)), 74.92 (**i**, (2, 4)). CH carbons, H−H region: 73.60 (**ii/ss**, (5, 7)), 73.20 (**is** + **si**, (5, 7)), 73.13 (**i**, (3, 6)), 73.01 (**ii/ss**, (5, 7)), 72.75 (**s**, (3, 6)). CH_2 carbons, T−T region: 76.06, 76.01, 75.81 (is/si/ii, (11, 14)), 75.70 (ss, (11, 14)), 75.44 (i, (10, 12)), 75.35 (s, (10, 12)). CH_2 carbons, H−T: 74.62 (ss, (13, 15)), 74.09 (ii, (13, 15)), 73.85 (is+is, (13, 15)), 73.47 (i, (9, 16)), 73.23 (s, (9, 16)). CH_3 carbons: 18.53, 18.36, 17.41, 17.29.

MS data: all peaks reported correspond to Cl−[(C_3H_6O)$_n$]−K^+ ions. Peak at m/z = 1237 for n = 20, m/z = 1295 for n = 21, m/z = 1411 for n = 23, m/z = 1586 for n = 26, m/z = 1702 for n = 28, m/z = 1818 for n = 30, m/z = 2109 for n = 35, m/z = 2284 for n = 38, m/z = 2342 for n = 39.

rac-PO/[($C_{23}H_{30}O_2$)AlCl]$_2$. Same procedure as above; see Table 10.

DEPT NMR (C_6D_6, δ, ppm, (tacticity, regiosequence)): CH carbons, H−T region: 75.80 (**ii**, (1, 8)), 75.70 (**si** + **is**, (1, 8)), 75.56 (**ss**, (1, 8)), 75.45 (**s**, (2, 4)), 75.30 (**i**, (2, 4)). CH carbons, H−H region: 73.65 (ii/ss, (5, 7)), 73.20 (is + si, (5, 7)), 73.12 (i, (3, 6)), 73.03 (ii/ss, (5, 7)), 72.81 (s, (3, 6)). CH_2 carbons, T−T region: 76.55, 76.47, 76.17 (is/si/ii, (11, 14)), 76.10 (ss, (11, 14)), 75.80 (i, (10, 12)), 75.70 (s, (10, 12)). CH_2 carbons, H−T: 74.60 (ss, (13, 15)), 74.12 (ii, (13, 15)), 73.90 (si +is, (13, 15)), 73.35 (i, (9, 16)), 73.20 (s, (9, 16)). CH_3 carbons: 18.50, 18.40, 17.51, 17.30.

S-PO/[($C_{30}H_{44}O_2$)AlCl]$_2$. The catalyst (0.05 g, 0.05 mmol) was added to *S*-PO (0.29 g, 350 μL), giving a solution with a ratio of catalyst:monomer of 1:100. After 48 h, the remaining monomer and other volatile species were evaporated under vacuum.

DEPT NMR (C_6D_6, δ, ppm, (tacticity, regiosequence)): CH carbons, H−T region: 75.49 (**ii**, (1, 8)), 75.10 (**s**, (2, 4)). CH carbons, H−H region: 73.21 (**is** + **si**, (5, 7)), 72.83 (**s**, (3, 6)). CH_2 carbons, T−T region: 75.76 (ss, (11, 14)), 75.43 (s, (10, 12)). CH_2 carbons, H−T: 73.92 (is + si, (13, 15)), 73.51 (i, (9, 16)). CH_3 carbons: 18.57, 18.39, 17.99, 17.40.

50% rac-PO/50% S-PO/[($C_{30}H_{44}O_2$)AlCl]$_2$. 0.5 mL of *S*-PO was mixed with 0.5 mL of *rac*-PO. The catalyst (0.14 g, 0.14 mmol) was added to this solution to give a ratio of catalyst: monomer of 1:100. After 72 h, the excess monomer and any other volatile species were removed under vacuum, and a yellow polymer was obtained.

DEPT NMR (C_6D_6, δ, ppm, (tacticity, regiosequence)): CH carbons, H−T region: 75.51 (**ii**, (1, 8)), 75.40 (**si** + **is**, (1, 8)), 75.27 (**ss**, (1, 8)), 75.11 (**s**, (2, 4)), 74.95 (**i**, (2, 4)). CH carbons, H−H region: 73.57 (ii/ss, (5, 7)), 73.25 (is + si, (5, 7)), 73.21 (i, (3, 6)), 73.15 (ii/ss, (5, 7)), 72.79 (s, (3, 6)). CH_2 carbons, T−T region: 76.10, 76.07, 75.85 (is/si/ii, (11, 14)), 75.75 (ss, (11, 14)), 75.44 (i, (10, 12)), 75.40 (s, (10, 12)). CH_2 carbons, H−T: 74.71 (ss, (13, 15)), 74.16 (ii, (13, 15)), 73.92 (is + is, (13, 15)), 73.53 (i, (9, 16)), 73.27 (s, (9, 16)). CH_3 carbons: 20.20, 18.50, 18.39, 17.95, 17.50, 17.43.

rac-PO/[($C_{24}O_2H_{32}$)AlX(THF)] (X = Cl, Ethyl). 0.01 g of catalyst (0.02 mmol) was added to 0.5 mL of *rac*-PO (7.1 mmol); ratio of catalyst:monomer 1:340. After stirring for 72 h, the excess monomer and any other volatiles species were evaporated under vacuum to give a colorless polymer.

DEPT NMR (C_6D_6, δ, ppm, (tacticity, regiosequence)): CH carbons, H−T region: 75.49 (**ii**, (1, 8)), 75.39 (**si** + **is**, (1, 8)), 75.25 (**ss**, (1, 8)), 75.09 (**s**, (2, 4)), 74.98 (**i**, (2, 4)). CH carbons, H−H region: 73.66 (**ii/ss**, (5, 7)), 73.53 (**is** + **si**, (5, 7)), 73.24 (**i**, (3, 6)), 73.04 (**ii/ss**, (5, 7)), 72.79 (**s**, (3, 6)). CH_2 carbons, T−T region: 76.12, 76.05, 75.85 (is/si/ii, (11, 14)), 75.75 (ss, (11, 14)), 75.49 (i, (10, 12)), 75.40 (s, (10, 12)). CH_2 carbons, H−T: 74.16 (ii, (13, 15)), 73.93 (is + is, (13, 15)), 73.54 (i, (9, 16)), 73.23 (s, (9, 16)). CH_3 carbons: 18.58, 18.41, 18.20, 17.47.

S-PO/[($C_{24}O_2H_{32}$)AlX(THF)] (X = Cl, Ethyl). 0.01 g of catalyst (0.02 mmol) were added to 0.5 mL of *S*-PO (7.1 mmol), with a ratio of catalyst:monomer of 1:340. After stirring for 72 h, the excess of monomer and any other volatile components were evaporated under vacuum to give a colorless polymer.

DEPT NMR (C_6D_6, δ, ppm, (tacticity, regiosequence)): CH carbons, H−T region: 75.48 (**ii**, (1, 8)), 75.08 (**s**, (2, 4)). CH carbons, H−H region: 73.24 (**is** + **si**, (5, 7)), 72.78 (**s**, (3, 6)). CH_2 carbons, T−T region: 75.74 (**ss**, (11, 14)), 75.39 (**s**, (10,

12)). CH_2 carbons, H−T: 73.91 (**is** + **si**, (13, 15)), 73.51 (**i**, (9, 16)). CH_3 carbons: 17.55, 18.41, 18.60.

50% rac-PO/50% S-PO/[($C_{24}O_2H_{32}$)AlX(THF)] (X = Cl, Ethyl). 0.4 mL of *S*-PO were mixed with 0.4 mL of *rac*-PO. The catalyst (0.059 g, 0.071 mmol) was added to this solution to give a ratio of catalyst:monomer (1:160). After 72 h, the excess monomer and volatile species were removed under vacuum, and a yellow polymer was obtained.

DEPT NMR (C_6D_6, δ, ppm, (tacticity, regiosequence)): CH carbons, H−T region: 75.57 (**ii**, (1, 8)), 75.38 (**si** + **is**, (1, 8)), 75.29 (**ss**, (1, 8)), 75.13 (**s**, (2, 4)), 74.98 (**i**, (2, 4)). CH carbons, H−H region: 73.60 (ss/ii, (5, 7)), 73.25 (is + si, (5, 7)), 73.19 (i, (3, 6)), 73.16 (ss/ii, (5, 7)), 72.80 (s, (3, 6)). CH_2 carbons, T−T region: 76.10, 76.04, 75.80 (is/si/ii, (11, 14)), 75.77 (ss, (11, 14)), 75.40 (i, (10, 12)), 75.38 (s, (10, 12)). CH_2 carbons, H−T: 74.71 (ss, (13, 15)), 74.18 (ii, (13, 15)), 73.96 (si+is, (13, 15)), 73.55 (i, (9, 16)), 73.30 (s, (9, 16)). CH_3 carbons: 20.30, 18.54, 18.39, 17.85, 17.56, 17.43.

PO/[($C_{30}H_{44}O_2$)AlO^{i}Pr]$_2$. The catalyst (0.03 g, 0.028 mmol) was added to 0.5 mL of PO (7.15 mmol). The mixture was left stirring at room temperature for a week and then sent to be analyzed by GPC/MS.

rac-PO/(TPP)AlCl. (TPP)AlCl (0.1 g, 0.16 mmol) was added to 5 mL of *rac*-PO, with a ratio catalyst:monomer of 1:430. Heat evolution during reaction was observed. Polymerization went to completion in 24 h, yielding a purple solid.

^{13}C NMR (C_6D_6, δ, ppm): 76.05 (CH, **ii**), 76.00 (CH, **is** + **si**), 75.80 (CH, **ss**), 74.12 (CH_2, **ii** + **is/ii** + **si**), 73.80 (CH_2, **ss**), 73.75 (CH_2, **is/si**), 17.86 (CH_3).

The same polymerization was done using methylene chloride as a solvent. No significant change with respect to the polymer microstructure obtained in bulk polymerizations was observed.

S-PO/(TPP)AlCl. (TPP)AlCl (0.1 g, 0.16 mmol) was added to 1 mL of *S*-PO. Ratio of catalyst:monomer (1:90). Heat of reaction was observed. Polymerization went to completion.

^{13}C NMR (C_6D_6, δ, ppm): 75.82 (CH, **ii**), 73.84 (CH_2, **i**), 17.83 (CH_3).

rac-PO/Calcium Amide−Alkoxide Catalyst. 10 mg of the calcium amide−alkoxide catalyst were added to 1 mL of *rac*-PO. After 24 h, the excess monomer was evaporated under vacuum.

^{13}C NMR (C_6D_6, δ, ppm): 75.86 (**ii**, CH), 75.73 (**is** + **si**, CH), 75.6 (**ss**, CH), 73.9 (**i**, CH_2), 73.7 (**s**, CH_2), 17.9 (CH_3).

rac-PO/KOH. KOH (0.01 g, 0.18 mmol) was added to 2 mL of toluene. This solution was added to 1 mL of *rac*-PO, giving a ratio catalyst:monomer of 1:80. After 24 h, polymerization was completed.

^{13}C NMR (C_6D_6, δ, ppm): 75.8 (CH, **ii**), 75.73 (CH, **is** + **si**), 75.6 (CH, **ss**), 73.86 (CH_2, **i**), 73.60 (CH_2, **s**), 17.87, 17.79 (CH_3).

rac-PO/Tin Tetrachloride. $SnCl_4$ (0.25 g, 0.07 mmol) was added to 4 mL of *rac*-PO (0.071 mol), with a ratio catalyst: monomer of 1:100. The formation of white fumes and local heat of reaction were observed. After 2 h, polymerization was completed.

^{13}C NMR (C_6D_6, δ, ppm): very broad peak with main peaks at 71, 64.50, 62.37, 61.14, 59.9 (CH), 28.29, 26.38, 22.78, 21.51, 20.06 (CH_3).

S-PO/BF_3:Etherate. 50 μL of BF_3:etherate were syringed to 1 mL of *S*-PO, with a ratio catalyst:monomer of 1:50. After 3 h, polymerization was completed.

^{13}C NMR (C_6D_6, δ, ppm): broad peaks with main peaks 75.24, 74.74, 72.18, 71.36, 66.33 (CH), 17.25, 16.29, 15.62, 14.55 (CH_3).

rac-PO/[$Cp_2Zr(OEt_2)(OEt)]^+[HB(C_6F_5)_3]^-$. The catalyst (0.07 g, 0.082 mmol) was added to 1.5 mL of PO (0.021 mol). After 10 min, polymerization was completed. NMR data are available in the Supporting Information.

The same procedure was done for the polymerization of *S*-PO.

Acknowledgment. We thank the Department of Energy, Basic Energy Sciences Chemistry Division, for financial support of this work at Indiana University. We also thank Professor Sheldon G. Shore and his group for the donation of a sample of $[Cp_2Zr(OEt_2)(OEt)]^+$-$[HB(C_6F_5)_3]^-$. B.A. thanks DAAD for a postdoctoral fellowship. We also thank the reviewers for their constructive comments.

Supporting Information Available: X-ray crystal structure determination and CIF data for compounds [($C_{30}H_{44}O_2$)-$AlCl]_2$ (**1**), [($C_{30}H_{44}O_2$)AlCl(THF)] (**3**), [($C_{24}H_{32}O_2$) $AlCl_{0.2}$ethyl$_{0.8}$-(THF)] (**4**), and [($C_{24}H_{32}O_2$) $AlCl]_2$ (**6**); spin−lattice relaxation time (T_1) measurements from ^{13}C NMR of the polymers obtained from reaction between *rac*-PO and [($C_{30}H_{44}O_2$)$AlCl]_2$, *S*-PO and [($C_{30}H_{44}O_2$)$AlCl]_2$ and *rac*-PO and [($C_{23}H_{30}O_2$)$AlCl]_2$ (**2**) as well as the corresponding deconvolution experiments and statistical calculations for the regioirregular sequences of the copolymer obtained from a mixture of 50% *rac*-PO and 50% *S*-PO; and DEPT NMR spectra for both *rac*-PO and *S*-PO polymerized with $[Cp_2Zr(OEt_2)(OEt)]^+[HB(C_6F_5)_3]^-$ as well as the GPC trace and MS data for the polymers obtained with this system. This material is available free of charge via the Internet at http://pubs.acs.org.

References and Notes

(1) Chisholm, M. H.; Eilerts, N. W.; Iyer, S. S.; Huffman, J. H.; Packold, M.; Phomphrai, K. *J. Am. Chem. Soc.* **2000**, 11845−11854.

(2) Brintzinger, H. H.; Fischer, D.; Mulhaupt, R.; Rieger, B.; Waymouth, R. M. *Angew. Chem., Int. Ed. Engl.* **1995**, *34*, 1143−1170. (b) Shapiro, P. J.; Schaeffer, W. P.; Labinger, J. A.; Bercaw, J. E.; Cotter, W. D. *J. Am. Chem. Soc.* **1994**, *116*, 4623−4640. (c) Scollard, J. D.; McConville, D. H. *J. Am. Chem. Soc.* **1996**, *118*, 10008−100009. (d) Coates, G. W.; Waymouth, R. M. *Science* (*Washington, D.C.*) **1995**, *265*, 217−219. (e) Coates, G. W. *Chem. Rev.* **2000**, *100*, 1223−1252.

(3) Duda, A.; Penczec, S. *Macromolecules* **1990**, *23*, 1636−1639. (b) Nijenhuis, A. J.; Grijpma, D. W.; Pennings, A. J. *Macromolecules* **1992**, *25*, 6419−6424. (c) Kricheldorf, H. R.; Beri, M.; Schmarnalg, N. *Macromolecules* **1988**, *21*, 286−293. (d) Trofimoff, L.; Aida, T.; Inoue, S. *Chem. Lett.* **1987**, 991−994. (e) McLain, S. J.; Ford, T. M.; Drysdale, N. E.; Jones, N.; McCord, E. F.; Shreeve, J. L.; Evans, W. J. *Polym. Prepr.* (*ACS Div. Polym. Chem.*) **1994**, *35* (2), 534−535.

(4) McLain, S. J.; Ford, T. M.; Drysdale, N. E.; Jones, N.; McCord, E. F.; Shreeve, J. L.; Evans, W. J. *Polym. Prepr.* (*ACS Div. Polym. Chem.*) **1994**, *35* (2), 534−535.

(5) Tsuruta, T.; Kawakami, Y. *Comprehensive Polymer Science*, Allen and Bevington Ed., 1st ed.; Pergamon Press: New York, 1989; Vol. 3, Chapter 31, pp 457−487. (b) Vandenberg, E. J. *J. Polym. Sci., Polym. Chem. Ed.* **1969**, *7*, 525.

(6) March, J. *Advanced Organic Chemistry*, 3rd ed.; John Wiley & Sons: New York, 1985; p 326.

(7) Inoue, S.; Sugita, T.; Kiso, Y.; Ichikawa, K. *Bull. Chem. Soc. Jpn.* **1976**, *49*, 9, 1063−1071.

(8) Takeda, N.; Inoue, S. *Makromol. Chem.* **1982**, *183*, 1383. (b) Aida, T.; Inoue, S. *Macromolecules* **1981**, *14*, 1162−1166.

(9) Le Borgne, A.; Spassky, N.; Lin Jun, C.; Momtaz, A. *Makromol. Chem.* **1988**, *189*, 637−650. (b) Sugimoto, H.; Kawamura, C.; Kuroki, M.; Aida, T.; Inoue, S. *Macromolecules* **1994**, *27*, 2013−2018.

(10) Aida, T.; Inoue, S. *Macromolecules* **1981**, *14*, 1166−1169.

(11) Shimasaki, K.; Aida, T.; Inoue, S. *Macromolecules* **1987**, *20*, 3076−3080.

(12) Isoda, M.; Sugimoto, H.; Aida, T.; Inoue, S. *Macromolecules* **1997**, *30*, 57−62. (b) Sugimoto, H.; Kamamura, C.; Kuroki, M.; Aida, T.; Inoue, S. *Macromolecules* **1994**, *27*, 2013−2018.

(13) Ramey, K. C.; Field, N. D. *Polym. Lett.* **1964,** *2*, 461−463. (b) Bruch, M. D.; Bovey, F. A.; Cais, R. E.; Noggle, J. H. *Macromolecules* **1985**, *18*, 1253−1257. (c) Abe, A.; Hirano, T.; Tsuji, K.; Tsuruta, T. *Macromolecules* **1979**, *12*, 1100−1107. (d) Hasebe, Y.; Tsuruta, T. *Makromol. Chem.* **1987**, *188*, 1403−1414. (e) Kasperczyk, J.; Jedlinsli, Z. J. *Makromol. Chem.* **1986**, *187*, 2215−2221. (f) Lindfors, K. R.; Pan, S.; Dreyfuss, P. *Macromolecules* **1993**, *26*, 2919−2927.

(14) Bovey, F. A.; Nirau, P. A. *NMR of Polymers*; Academic Press: San Diego, 1996. (b) Koenig, J. L. *Chemical Microstructure of Polymer Chains*; Wiley-Interscience Publication; John Wiley and Sons: New York, 1980. (c) Bovey, F. A. *Comprehensive Polymer Science*, 1st ed.; Pergamon Press: New York, 1989; Vol. 1, Chapter 17. (d) Bruch, M. D. *NMR Spectroscopy Techniques*, 2nd ed.; M. Dekker: New York,

1996. (e) Bruch, M. D.; Bovey, F. A.; Cais, R. E.; Noggle, J. H. *Macromolecules* **1985**, *18*, 1253.
(15) Landau, R.; Sullivan, G. A.; Brown, D. *ChemTech* **1979**, *October Issue*, 602−607. (b) Ultree, A. J. *Encyclopedia of Polymer Science and Engineering;* John Wiley and Sons: New York, 1986; Vol. 6, pp 733−755.
(16) POLYOX Resin Flocculants for the Mining industry, Technical Bulletin F-45950, Union Carbide Corporation, New York, 1976. (b) POLYOX Water Soluble Regions Control Flow of Cleaning Solutions, Technical Bulletin F-42939, Union Carbide Corporation, New York, 1974.
(17) Ultree, A. J. *Encyclopedia of Polymer Science and Enginneering;* John Wiley and Sons: New York, 1986; Vol. 6, pp 733−755. (b) Bolick, J. E.; Jensen, A. W. In *Encyclopedia of Chemical Technology*, 4th ed.; Kirk-Othmer, Ed.; John Wiley and Sons: New York, 1993; Vol. 10, pp 624−638.
(18) Gan, Z.; Jim, T. F.; Li, M.; Yuer, Z.; Wang, S.; Wu, C. *Macromolecules* **1999**, *32*, 590−594. (b) Aida, T.; Inoue, S. *Macromolecules* **1981**, *14*, 1162−1166. (c) Aida, T.; Inoue, S. *J. Am. Chem. Soc.* **1985**, *107*, 1358−1364.
(19) Goeke, G. L.; Park, K.; Karol, P. J.; Mead, B. U.S. Patent 4,193,892, Union Carbide, 1980.
(20) Schrock, R. R. *Acc. Chem. Res.* **1990,** *23*, 158−165.
(21) Schilling, F. C.; Tonelli, A. E. *Macromolecules* **1986**, *19*, 1337−1343.
(22) Atwood, D. A.; Jegier, J. A.; Rutherford, D. *J. Am. Chem. Soc.* **1995**, *117*, 6779−6780. (b) Atwood, D. A.; Jegier, J. A.; Rutherford, D. *Inorg. Chem.* **1996**, *35*, 63−70.
(23) Chisholm, M. H.; Huang, J.; Huffman, J. C.; Streib, W. E.; Tiedtke, D. *Polyhedron* **1997**, *16*, 2941−2949.
(24) Ko, B.; Wu, C.; Lin, C. *Organometallics* **2000**, *19*, 1864−1869.
(25) Liu, F. C.; Liu, J.; Meyers, E. A.; Shore, S. G. *J. Am. Chem. Soc.* **2000**, *122*, 6106−6107.
(26) Tsuruta, T.; Kawakami, Y. *Comprehensive Polymer Science*, Allen and Bevington Ed., 1st ed.; Pergamon Press: New York, 1989; Vol. 3, Chapter 33, pp 489−500. (b) Tsuruta, T. *Makromol. Chem., Macromol. Symp.* **1986**, *6*, 23−31. (c) Tsuruta, T. *Makromol. Chem., Rapid Commun.* **1984**, *5*, 89.
(27) Tonelli, A. E.; Schilling, F. C. *Acc. Chem. Res.* **1981**, *14*, 233.
(28) Challa, G. *Polymer Chemistry. An Introduction*, Ellis Horwood Series in Polymer Science; Ellis Horwood Limited: Chichester, 1993; pp 96−98.
(29) Cheng, M.; Attygalle, A. B.; Lobkovsky, E. B.; Coates, G. W. *J. Am. Chem. Soc.* **1999**, *121*, 11583−11584.
(30) Chisholm, M. H.; Huffman, J. C.; Navarro-Llobet, D., unpublished results.
(31) Chisholm, M. H.; Huffman, J. C.; Phomphrai, K. *J. Chem. Soc., Dalton Trans.* **2001**, 222−224.

MA0102316